AD-750 468

CRUSTAL DEFORMATION PROPAGATION

Eduard Berg

Alaska University

Prepared for:

Air Force Office of Scientific Research
Advanced Research Projects Agency

September 1972

GEOPHY E

UNIVERSITY OF ALASKA

COLLEGE, ALASKA

UAG R-222

CRUSTAL DEFORMATION PROPAGATION

by

Eduard Berg

September 1972

FINAL REPORT

Contract F-44620-71-C-0105

Sponsored by

Air Force Office of Scientific Research
Advanced Research Projects Agency
ARPA Order No. 1827

56

Unclassified

Security Classification

DOCUMENT CONTROL DATA - R & D

(Security classification of title, body of abstract and indexing annotation must be entered when the overall report is classified)

1. ORIGINATING ACTIVITY (Corporate author) Geophysical Institute University of Alaska Fairbanks, Alaska 99701	2a. REPORT SECURITY CLASSIFICATION Unclassified 2b. GROUP

3. REPORT TITLE

CRUSTAL DEFORMATION PROPAGATION

4. DESCRIPTIVE NOTES (Type of report and inclusive dates)

Scientific, Final September 1972

5. AUTHOR(S) (First name, middle initial, last name)

Eduard Berg

6. REPORT DATE	7a. TOTAL NO. OF PAGES	7b. NO. OF REFS
September 1972	56	15

8a. CONTRACT OR GRANT NO. F44620-71-C-0105 b. PROJECT NO. AO 1827 c. 62701D d. --	9a. ORIGINATOR'S REPORT NUMBER(S) UAG R-222 9b. OTHER REPORT NO(S) (Any other numbers that may be assigned this report) AFOSR - TR - 72 - 1977

10. DISTRIBUTION STATEMENT

Approved for public release, distribution unlimited.

11. SUPPLEMENTARY NOTES	12. SPONSORING MILITARY ACTIVITY
Tech, Other	Air Force Office of Scientific Research (NPG 1400 Wilson Boulevard Arlington, Virginia 22209

13. ABSTRACT

Tilt steps similar to strain steps have been observed for earthquakes with magnitudes ranging from 2 to 8 and distances ranging anywhere from 10 km to 12,600 kilometers. Tilt-step propagation velocities from the hypocenter to the station have been observed from 1.2 to 3.8 km/sec, and those corresponding to the arrival time of teleseismic S waves. Tilt directions, amplitudes and velocities observed at several stations simultaneously for the same earthquake are internally consistent and are likely to depend on the tectonic environment of the station in addition to the focal mechanism. The low velocity of 1.2 km/sec is consistent with a plastic wave propagation. Other velocities are close to the Rayleigh wave short-period group velocity over continental paths.

DD FORM 1 NOV 65 1473

Unclassified

Security Classification

14 KEY WORDS	LINK A		LINK B		LINK C	
	ROLE	WT	ROLE	WT	ROLE	WT
ALASKA						
Seismicity - Geology						
Tilt - Propagation Velocities						
Amplitudes, Directions						
Plastic Deformation Propagation						
ALPA (Alaska Long-period Array)						

ii

Unclassified
Security Classification

GEOPHYSICAL INSTITUTE

of the

UNIVERSITY OF ALASKA

Final Report

CRUSTAL DEFORMATION PROPAGATION

by

Eduard Berg

Sponsored by

Air Force Office of Scientific Research
Contract F-44620-71-C-0105

Advanced Research Projects Agency
ARPA Order No. 1827

September 1972

Principal Investigator

Eduard Berg
Professor of Geophysics

Approved by:

Keith B. Mather
Director
Geophysical Institute

1C

GEOPHYSICAL INSTITUTE

of the

UNIVERSITY OF ALASKA

AFOSR Contract No. F 44620-71-C-0105
Project Title: Crustal Deformation Propagation
ARPA Order No. 1827
ARPA Program Code No. 1F10
Starting Date: 1 May 1971
Termination Date: 31 May 1972
Amount of Contract: $79,000
Project Scientist: Dr. Eduard Berg
Geophysical Institute
University of Alaska

(Now at the Hawaiian Institute of Geophysics
University of Hawaii
Telephone Number: 808-944-8762)

id

TABLE OF CONTENTS

PERSONNEL

The program of research described in these pages would not have been possible without the interest, dedication and professional competence of the members of the seismological laboratory. The principal investigator wishes to express his gratitude and thanks to all.

Dr. Nirendra Biswas, Assistant Professor

Dr. Hans Pulpan, Assistant Professor

Larry Gedney, Associate Geophysicist

Douglas VanWormer, Assistant Geophysicist

John Davies, Senior Research Assistant

William Lutschak, Senior Research Assistant

Ronald Rasmussen, Engineer

Orwin Westwick, Engineering Aide

Ingrid Gwalthney, Data Analyst

ACKNOWLEDGMENTS

Thanks and appreciation are expressed to Mr. William Best, Chief, Geophysics Division, AFOSR, for his continued interest and support which made this program possible. The efficient help of the Alaskan Air Command and RCA is acknowledged for the continued maintenance of communication links for the telemetry system and for helicopter support in the Skwentna operation. Thanks go to the NASA STADAN station director, Ed Eisele, for permission to operate and maintain the Gilmore (CLM) borehole station and for frequent help and permission to use a data-link. Thanks are expressed to Judge Hepp for the continuous and general permission to operate a short-period telemetry station (HPP) on his property.

Finally, appreciation is expressed for providing seismic records and other information to the following persons: Mr. Hartemberger, Geotech, Alexandria Laboratories; Mr. Howard Butler, NOAA Tsunami Warning Network, Palmer; Mr. Jack Townshend, NOAA, College Observatory; Dr. Maurice Major, Colorado School of Mines.

ABSTRACT

During the contract period the main emphasis was on the observation of crustal tilts associated with earthquakes, their directions, amplitudes and propagation velocities. Data from the seismology laboratory's three borehole installations at GLM, PAX, MCK, the COL World Wide Standard Station and the ALPA (Alaska Long Period Array) have been analyzed for tilt steps associated with local earthquakes. Tilt steps from distant earthquakes observed at GLM, PAX and MCK and data presented in the literature are discussed. Observed tilt steps cover a distance range from 8 to 12600 km and a magnitude range from 2 to 8. Tilt step propagation velocities have been observed from 1.2 to 4.0 km/sec, and those corresponding to arrival times of teleseismic S waves. Tilt directions, amplitudes and velocities observed at several stations simultaneously for the same earthquake are internally consistent and are likely to depend on the tectonic environment of the observing station in addition to the focal mechanism. The low velocity of 1.2 km/sec is consistent with a plastic wave propagation. Other velocities are close to the Rayleigh wave short-period group velocity. The tilt amplitude for fixed epicenter distance, focal depth and stress system depends logarithmically on the magnitude, with a possible cut-off, but are too large when compared to existing theoretical dislocation models for a single layered homogeneous isotropic elastic crust. Alternative solutions in terms of more realistic crustal layering and including plastic deformation under preexisting tectonic stress probably could account for a number of observations.

The operation of a number of short-period telemetry stations has been discontinued, new ones installed and one was relocated.

A seismicity map was published for the period 1968-1971, based on recordings from the telemetry net and the results related to the geology of Alaska. The map and its geology related discussion proved very useful to a number of state agencies (such as the Highways Department) and aroused much interest from private sources as well.

TELEMETRY NETWORK

A number of changes in the telemetry network have been made during the contract period. The operation of BIG, PJD, SVW and BLR have been discontinued. MCB was replaced by ENG, and CCB and FYU have been newly established. The following table indicates all seismic stations operated by the Geophysical Institute, though not all under this contract or by the seismology laboratory.

Station Name	Code	Latitude (N)	Longitude (W)	Elevation	Components
Augustine Island	AGI	59 22.8	153 25.2	580	SPZ
Broad Pass	BDP	63 13.87	149 15.56	709	SPZ
Birch Hill	BRH	64 51.89	147 38.42	330	SPZ
Clear Creek Butte	CCB	64 38.88	147 48.32	183	SPZ
Elvey	ELV	64 51.62	147 50.91	180	SPZ Low Gain
Engineer Hill	ENG	64 44.11	147 02.76	220	SPZ
Fort Yukon	FYU	66 33.96	145 13.90	137	SPZ
Gilmore	GLM	64 59.24	147 23.34	820	SPZ, LP, Tilt
Hepp	HPP	64 47.43	147 57.55	170	SPZ
Hurricane	HUR	62 58.74	149 38.77	510	SPZ
McKinley	MCK	63 43.94	148 56.1	610	SPZ, LP, Tilt
Mercer	MCR	63 53.71	149 0[illegible].56	456	SPZ
Minitrack	MIK	64 52.34	147 49.68	160	SPZ
Nenana	NEA	64 34.63	149 04.63	365	SPZ
Paxson	PAX	62 58.25	145 28.12	1130	SPZ, LP, Tilt
Remote	RON	62 41.47	150 12.22	470	SPZ
Sheep Mtn	SCM	61 50.00	147 19.66	1020	SPZ
Sunshine	SSH	62 10.00	150 04.66	100	SPZ
Scotty Lake	SCT	62 19.15	150 17.83	140	SPZ
Tanana	TNN	65 15.4	151 54.7	504	SPZ

EARTHQUAKE EPICENTERS IN INTERIOR ALASKA, 1968-1971

Contribution by L. Gedney, L. Shapiro, D. VanWormer and F. Weber*

On the accompanying map, somewhat over 1500 epicenters are represented. These data were collected by the Geophysical Institute's telemetered seismic net during the four-year period 1968-1971, and the calculations giving the earthquake parameters were performed by the University of Alaska's IBM 360-40 computer. No distinction is made as to earthquake magnitude, although it is likely that none smaller than magnitude 2 are depicted, and that the heaviest concentrations represent aftershock zones of larger earthquakes. An exception to the latter statement is the dense concentration in the Mt. McKinley area (63°N, 151°W), where very many small, intermediate depth earthquakes occur, but earthquakes of over magnitude 5-1/2 are rare. Other clusters of note occur at: 64.6°N, 147.0°W, the area of the Salcha earthquake of July 1937 (m = 7-1/4); 64.8°N, 147.4°W, the aftershock zone of the Fairbanks earthquakes of June 1967 (m = 6-1/4); and 65.5°N, 150.0°W, the aftershock zone of the Rampart earthquake of October 1968 (m = 6-1/2).

The correlation of epicenters with mapped faults is clear in the case of the Rampart Fault, the Denali Fault (extending east to west across the bottom of the map), and several faults of lesser magnitude. It appears likely that unmapped faults may exist in other areas where obvious epicentral alignment occurs, particularly in the Fairbanks area.

* U. S. Geological Survey

CRUSTAL STRUCTURE AND PLATE TECTONICS NEAR THE WESTERN PART OF THE ALASKA RANGE

Contribution by John Davies and Eduard Berg

As part of a continuing program of crustal studies in Alaska, 5 temporary, VHF telemetered, seismic stations were operated at the base of the Alaska Range in the vicinity of Skwentna (about 120 km NW of Anchorage), Alaska, during June and July 1971. All of the stations were installed and maintained using USAF helicopters from Elmendorf, Alaska. The station sites were chosen to increase the precision with which earthquake hypocenters could be located in the subduction zone NW of Anchorage along the Alaska Range. The stations augmented those operated routinely by the Geophysical Institute, University of Alaska, and the Palmer Seismological Observatory, NOAA.

Data from these three sources is now being analyzed and preliminary results promise that this project will succeed in refining previous work on dipping crust-mantle interface and tectonics of the Cook Inlet-Susitna River region, and be the basis for further seismological studies in the area. It is important to understand the seismicity of this region since half the population of the State of Alaska lives in it.

This project was significant because it marked the first extensive field use of VHF telemetry in seismic recording by our group. The experience gained is now being used in other areas of the State as we are operating about 10 VHF telemetered seismic stations. The advantages of this kind of system are many in a region where stations are needed in remote locations without roads, telephone channels or power.

CRUSTAL TILT FIELDS AND PROPAGATION VELOCITIES ASSOCIATED WITH EARTHQUAKES

Contribution by Edward Berg* and William Lutschak

ABSTRACT

Tilt steps similar to strain steps have been observed for earthquakes with magnitudes ranging from 2 to 8 and distances ranging anywhere from 10 km to 12,000 kilometers. Tilt-step propagation velocities from the hypocenter to the station have been observed from 1.2 to 3.8 km/sec, and those corresponding to the arrival time of teleseismic S waves. Tilt directions, amplitudes and velocities observed at several stations simultaneously for the same earthquake are internally consistent and are likely to depend on the tectonic environment of the station in addition to the focal mechanism. The low velocity of 1.2 km/sec is consistent with a plastic wave propagation. Other velocities are close to the Rayleigh wave short-period group velocity over continental paths.

*Now: Hawaiian Institute of Geophysics, University of Hawaii

INTRODUCTION

Tilt and strain steps associated with earthquakes have been observed widely. Their amplitudes often exceed those theoretically expected from elastic fields associated with a dislocation at the source. Observations on propagation velocities are sparse and mostly confined to a single path (Wideman and Major, 1967; Berg and Pulpan, 1971). Tilt (and strain) step amplitudes and velocities are presented for teleseisms traveling through different regions at near S- and Rayleigh-wave velocities, and for local earthquakes recorded at several stations simultaneously. Observations of some local earthquakes cover a full quadrant and should provide some understanding of near-source dynamics in relation to source and tectonic setting.

INSTRUMENTATION AND METHOD

The University of Alaska's Tripartite Tilt network at MCK, PAX and GLM has been presented by Berg and Pulpan (1971). The network is comprised of borehole installations of horizontal Lamont-Lunar type 15-second pendulums equipped with capacitor transducers. The HIG (21°18'05"N, 157°49'20"W) installation consists of NS and EW Sprengnether LP pendulums (at T_o = 20 seconds) mounted on a concrete pier in the basement of the institute building (Hawaii Institute of Geophysics). Output at the time of the earthquakes reported here was recorded to DC from a Sprengnether capacitor transducer on Helicorder paper. The ALPA installation north of Fairbanks consists of triaxial long-period (T_o = 20 seconds) borehole seismometers with velocity transducers and position monitor. Station locations are shown in figure 15. Only a limited amount of data has become available to far.

To determine amplitudes and velocities for teleseisms and regional events, either the digital records (1 data point/second) or the tidal outputs (both to DC) were used together with the epicenter and origin time of the U.S.C.G.S. preliminary or monthly determinations. Great circle path distances were determined through a geodetic computer program by Gary Schnelzer (Hawaii Institute of Geophysics). For the last two events in Table 1, arrival times were read from the records presented in the literature by Stacey and Rynn (1970) and Tocher and Brown (1971), and their tilt and strain steps and distances were used. (Those of Wideman and Major, 1967, were not.)

For local Fairbanks earthquakes, Berg and Pulpan (1971) presented a number of offset tidal records and the corresponding pulses on the LP outputs (including the 10 October 1970 earthquake for GLM). GLM is located inside ALPA. An analog output for a step input (Cal pulse) of one of the ALPA seismometers was obtained (lower left corner of Figure 15). If the records of local earthquakes from GLM showed tilts, and the pulses propagating through ALPA could be superimposed on the calibration pulse form, the corresponding output was considered to result from a tilt.

During the 9th International Symposium on Geophysical Theory on Computers the question was raised whether or not such a pulse output could result from the saturation of the ALPA seismic amplifiers by large amplitude short-period waves of the local earthquakes. However, this seems unlikely. In several cases the tilt only occurred in one direction, whereas the other perpendicular output shows only noise. As an example, consider the NS component of station 34 (Figure 14c) that only showed noise (trace 343). The output level corresponds to 3.73 x 10 = 37.3 mμ at the maximum system response (at 25 sec period, Table 2, Seismogram 114, Channel 343). Since this output is vectorially composed of the three outputs of the triaxial system it should show saturation at a much higher level (comparable to the pulse amplitude of the east-west output (Figure 14b) trace 342) if saturation of one or more amplifiers had taken place. Since it does not show such a saturation it is concluded that the pulse shown on the east-west output is real (Figure 14b, trace 342) corresponding to an output level of 2.2 μ at the maximum system response at 25 sec period (Table 2, seismogram 113, Channel 342). Similarly it is felt that the other pulses that are like a step input to the calibration coil (shown in the lower left of Figure 15) are real. In other cases the pulse is clearly visible but of smaller amplitude than the maximum noise level recorded during the time interval for which the record has been obtained (as station 36 for 12 November 1970, Figure 19).

For some ALPA outputs with responses deviating somewhat from the ideal step response, overshoot amplitudes were used to determine tilt amplitudes. Absolute tilt amplitudes were obtained by converting the given output amplitudes via calibration amplitudes (or voltages) and using $mg\sin\alpha \approx mg\alpha = iG$, where m = mass of seismometer, g earth gravity, α = deviation angle of seismometer boom for the equivalent pendulum length of a 20 sec pendulum when the calibration current i is applied and G is the calibration coil constant. Time resolution on the computer-plots was 1 inch/100 seconds for the 10 October 1970 and 12 November 1970 earthquakes and 2 inches/100 seconds for the others. Original computer outputs are presented in Figures 14 and 15 near corresponding station locations and are so oriented that ground motion N and E corresponds to record trace N and E. The corresponding tilt amplitude for the trace (normalized to $\pm$ 1 inch) is also shown. The resulting tilt direction and amplitude are presented in the figures. Results for COL have been similarly obtained.

Only those records that matched the calibration pulse have been used to determine the arrival times shown in Figure 10 for local quakes (exceptions or poor results for regional and distant earthquakes are given in brackets in Table 1).

Focal point and origin time have been determined from a local short-period telemeter network using the S-P times at LV and P arrivals at all other short-period stations (see Figures 15 to 19 for locations). S-P times at LV for the four earthquakes used in Figure 5 ranged from 1.8 to 3.7 seconds.

RESULTS

A) Distant and Regional Earthquakes

Tilt (and strain) amplitudes and propagation velocities for a distance range of 70 km to 12,600 km and a magnitude range of 3.6 to 8.0 are presented in Table 1. The velocities determined from arrivals on digital or Helicorder records should be considered very reliable, whereas those obtained from tidal records (25 mm/hour) are presented only as being indicative. Three rather distinct velocity groupings are apparent: that of 2.6 to 2.8 km/sec traveling through parts of the Aleutian arc (6 November 1971), South Central Alaska (26 March, 1971), and in an area north of Fairbanks (11 May 1971); that near 3.1 km/sec traveling at least partially through the continental area; and that of 3.5 to 3.8 km/sec traveling through the Pacific. All three types of step arrivals seem to be associated with and somewhat follow, in time, the maximum amplitudes of the Rayleigh waves. A fourth step arrival follows closely the S-wave arrival: it is visible on the Stacey and Rynn (1970, their Figure 1) illustration (17 January 1968) and on our digital and Helicorder records (10 January 1970, 29

February 1972). A tilt associated with the P-wave arrival might also be present in the Stacey and Rynn record.

It should be noted that tilt steps at PAX and MCK for the New Guinea and the Solomon Islands earthquakes (10 January 1971 and 14 July 1971, respectively) are nearly identical in direction and amplitude (Figures 5 and 6). The stations are nearly 200 km apart, along the Denali Fault in the Alaska Range, whereas at GLM, on the northern edge of the Tanana Basin 250 km away, the tilt steps show much smaller amplitudes, for roughly similar epicentral distance and azimuth. Both earthquakes also had comparable magnitudes.

The rise time of the tilt steps seems to be small when compared to seismometer and circuit time constants. Most of the tilt steps do not seem to recover with time. Figures 1 through 9 show typical tidal and digital records.

B) Local Earthquakes

Results of tilt-step arrival times versus focal distance are presented in Figure 10. The earthquake magnitudes ranged from 3.0 upward and depths were 18 to 20 km and 11 km (1 May 1971). Other observations not presented here include an earthquake of magnitude 2.4 and depth of 14 km, for which tilt steps were recorded at GLM and only at nearby ALPA stations.* Since the stations are very near the epicenters, focal distance-travel time served to calculate the step velocities.

---

*A magnitude 2 earthquake was the smallest, for which a tilt step (of 2 msec arc) has been observed at GLM.

Three groups of velocities are indicated: one of about 4 km/sec which includes the 3.6 km/sec (10 October 1970, because of relatively poor time resolution on the computer plots); a second of about 2.3 to 2.5 km/sec; and the third of 1.2 km/sec (13 May 1971). It should be noted that for the earthquake of 1 May 1971, stations 33, A2 and 32 are all aligned with the epicenter and GLM is only slightly off. If the 2.40 km/sec line through the arrivals at those stations is adjusted so as to pass 0 focal distance at a time different from the origin time, a better fit is obtained, resulting in a somewhat lower velocity near 2.2 km/sec.

Rise times on the ALPA output correspond (from visual matching by superposition) to that of a calibration step input, and at GLM are small compared to instrument and filter-time constants. For GLM this has also been verified for unfiltered digital outputs from local earthquakes (Figure 1).

C) Amplitude-Distance

The combined vectorial amplitude of the tilt steps for the ALPA, GLM and COL stations are presented for 7 earthquakes that originate near these stations. Figures 11a, b show tilt amplitudes versus epicentral distance; all data are summarized in Figure 12. Tilt amplitude and direction of 5 of the local quakes are presented in Figures 15 through 19. The numbers at the tip of the tilt arrow indicate the factor by which the length of the arrow has to be multiplied to obtain tilt amplitude corresponding to the scale in the right hand lower corner of the figures. Local magnitudes range from 2.8 to somewhat over four and have been determined from short-period vertical station LV, BLR and SCM. LV is located in the epicentral area, BLR is some 150 to 180 km and SCM over 300 km from the epicenters. Epicentral distance for the tilt steps recorded range from 8 to 80 km. Data points (tilt amplitude versus epicenter distance) in brackets indicate either possible maximum values (especially below 10 msec arc) or are doubtful. Stations indicated by the same subsymbol (vertical, horizontal or oblique line) are located on or nearly on a line passing through the epicenter indicated by a circle and cross in Figures 15 through 19. Amplitude die-off with distance R as R^{-x} is as indicated next to the lines joining corresponding in line stations. The value for x varies from 1.6 to over 7. For none of the 7 earthquakes all ALPA data have been obtained. However, in many instances stations did not show any pulse or other motion related to the earthquakes, out of the noise level. The noise level indicated by the output was lowest for the three northern most stations. Those stations that showed only noise are indicated in Figure 19 by an additional circle around the station location. There is doubt concerning the output of station 11 for the May 1971 quakes, showing exceedingly high amplitude, compared to surrounding stations or earlier earthquakes. The high amplitude is due to a single component of the triaxial system (aligned with the structural trends in the area), whereas the two other components show very small amplitudes on the raw data. A similar situation occurs, however, for other ALPA stations showing "reasonable" outputs, a fact that would argue for retention of data for the May 1971 quakes at station 11.

DISCUSSION

A) Distant and Regional Earthquakes

Maue (1954) has investigated (two dimensionally) the motion of relaxation that occurs when an elastic medium under tension (in y direction) is suddenly cut open from one side, perpendicular to the tension axis (along $x < 0$, $y = 0$). The plane compressional wave corresponding to a step is the strain ε_{yy} at the shockfront, and the amplitude is such that the initial tension is compensated. On the other hand, if a solution corresponding to a sinusoidal point force in a semi-infinite medium may be expressed as g (ω, coordinates, elastic and source parameters) $e^{i\omega t^*}$, where t* is the time corresponding to a particular propagation mode, and a step in force is applied at the source at t = 0, the resulting solution is given by the fourier integral over the fourier transform of the source time function times the solution function (Ewing et al., 1957, page 61) integrated over ω. Therefore a step in stress (and strain and tilts) is expected at the recording site at times corresponding to the particular propagation modes. The observations of steps traveling at velocities near S- and Rayeligh-wave velocities seem to confirm this contention.

Moreover, the velocities of steps occurring during the Rayleigh-wave train seem to correspond closely to the high-frequency portion of the continental Rayleigh waves group velocity (i.e., 3.1 km/sec), and for the local earthquakes, also close to the velocities of sedimentary Love and Rayleigh waves (2.0 - 2.5 km/sec) (Oliver, 1962). The velocities (Table 1) across parts of the Pacific closely correspond to those observed by Wideman and Major (1967) for oceanic paths.

The velocities of tilt (and strain) steps associated with the S waves correspond closely to the S-wave arrival time. Particularly noteworthy is the observation of a compressional strain in the NW-SE direction associated with such an S-wave arrival time from the Amchitka explosion at Cape Sarichef (record in Tocher and Brown, 1972). Calculations of the strain and tilt field resulting from a purely elastic dislocation model at the source have been carried out by different authors. However, the tilt amplitudes for the teleseismic events often exceed the theoretically expected ones by many times (as in Press, 1965). Moreover, there also are large amplitude differences among PAX and MCK on the one hand and GLM on the other for the New Guinea and the Solomon Island earthquakes for similar epicentral distance and azimuth. For a different azimuth (the Chile earthquake), however, amplitude differences (for comparable magnitudes) are much smaller at PAX, MCK and their relation to those at GLM is different. This supports Stacey and Rynn's idea that the tilt steps are related to local tectonics - in the Alaska case on a large scale, since the records for MCK and PAX near the Alaska Range are remarkably similar, whereas those at GLM north of the Tanana Basin are different (compare Figures 5 through 9). It is too early to compare the tilt-step direction to a local secular trend, because recording times are not long enough. A more detailed discussion of the amplitude fall-off with distance has been given in an earlier paper (Berg and Pulpan, 1971).

B) Local Earthquakes

Any discussion of the results of local earthquakes is a most ambiguous one since only one full quadrant of data for the deformation of the crustal material in the form of tilt steps and their arrival times is available, and theoretical calculations for surface deformation resulting from strike slip faulting at distances, comparable to source depth, and realistic velocity-depth functions are almost nonexistent.

(a) Tilt Direction

The assumption of almost vertical faults with strike slip motion resulting from a N- to NW-oriented, compressional axis in the area is supported by short-period and tilt investigations (Berg and Pulpan, 1971; Gedney and Berg, 1969a and 1969b). The tilt field directions of the 10 October 1970 earthquake (Figure 18) are consistent with theoretical calculations (Chinnery, 1961; Press, 1965) for a semi-infinite medium if the line for zero vertical uplift (that is roughly at a distance from the epicenter which is close to the focal depth) is placed beyond stations BRH and 33. In this case, all short-period first-motion observations (Berg and Pulpan, 1971) at MCK, HPP, LV, MIN, BRH, GLM and MCB are consistent, PJD actually showing only a small up-motion followed by a large down-motion, indicative of a location near the nodal plane. Of the ALPA stations, only station 34 shows a downward motion inconsistent with the interpretation, whereas the down-motion at station 23 and the up-motion at station 33 might result from nearness to the nodal line and/or a small dip in the nodal plane. The nodal planes required to fit this solution are nearly NS and EW, the NS plane passing slightly to the east of GLM, and the motion is either north on the eastern side of the NS plane or east on the northern side of the EW plane, consistent with a northeasterly compressional axis. It is believed that tilt-field directions would not be altered drastically if a realistic velocity-depth function were to be used in the theoretical calculations, and the amplitudes might be closer to observations. R. Sato (personal communication, April, 1972) has shown theoretically that the inclusion of a 1.7 km thick surface layer (V_p = 3.56, V_s = 2.37 km/sec) followed by a 2.8 km thick layer (V_p = 5.5, V_s = 3.10 km/sec) over higher velocity layers in the crust drastically alters the deformation surface field for dip-slip and inclined strike-slip dislocations, whereas numerical calculation for a model with a first layer of 33 km thickness (V_p = 6.3, V_s = 3.55 km/sec) results in surface deformation closely similar to that of a semi-infinite medium (Sato, 1971).

(b) Tilt Velocities

The arrival times most often observed for focal distances to 40 km correspond to a velocity of 2.0 to 2.3 km/sec. These might be interpreted as associated with the Rayleigh wave for a sedimentary layer at the edge of the Tanana Basin. Hanson et al. (1968) found such a layer 2.1 to 2.6 km thick (V_p = 3.67, V_s = 2.31 km/sec) at least to the edge of the basin. However, parts of the travel path are through Birch Creek schist and the interpretation is open to question. At larger distances (beyond 70 km) velocities near 2.8 to 3.1 km/sec have been observed corresponding to those for the pulses associated with Rayleigh waves over continental paths (see Figure 10, 13 May 1971, station 31).

No explanation is offered for the 4 km/sec branch which shows a delay of nearly 10 seconds for the 10 October 1970 and 16 January 1971 earthquakes, but no delay for the shallow-depth earthquake of 1 May 1971. A very low propagation velocity (1.2 km/sec) was observed between stations 33 and A2 (in line with the epicenter of the 13 May 1971 earthquake) and occasionally for arrivals at a single station (like that at station 24, 16 January 1971). The lowest velocity observed was 0.9 km/sec. Likewise Romig and others (1969, their Figure 3, site 2) seems to indicate a strain step arrival about 1 minute to 1 minute and 20 sec after the origin time of BENHAM at a distance of 71.5 km, indicating a similar low velocity of propagation near 1 km/sec. These low velocities seem to be associated with the propagation of a plastic pulse in a highly stressed area. By superposing the earthquake-generated stress, the nonlinear portion of the stress-strain curve is responsible for a plastic wave that will travel with a velocity V as given by Kolsky (1953):

$$V^2 = (\frac{d\sigma}{d\varepsilon} / \rho)$$

where σ = stress, ε = strain and ρ = density. In the linear part of the stress strain curve $d\sigma/d\varepsilon$ = E or Young's modulus. In the nonlinear part, for V = 1.2 km/sec and ρ = 2.7 gm/cm^3, a value of 3.9 x 10^{10} dyne/cm^2 is obtained for the modulus. This is twenty times lower than the corresponding

E modulus for a material with V_p = 5.5 km/sec. As a consequence, such a plastic wave will generate a considerably larger deformation than the elastic wave for the same applied stress. A plastic deformation could also be triggered by stresses from teleseismic sources in a prestressed area and could perhaps alter the direction of the tilt (and strain axis) and account for some of the larger tilt-amplitudes observed in tectonically active areas, such as the Alaska Range.

(c) Tilt Amplitudes

A number of features emerge from the data. Most of the local earthquakes are at a depth near 20 km, so that the theoretically strong dependence of deformation amplitudes on depth (like H^{-2}) is not considered in this discussion.

Tilt amplitudes for the same distance and magnitude scatter at least by an order of magnitude and seem dependent on station location. As an example, station 24 shows about one order less in amplitude (compared to other ALPA stations) for similar epicentral distance (Figure 12). Station 31 seems to indicate higher amplitudes (when recorded) that might be structurally controlled, indicated by the predominantly WSW tilt direction for the Fairbanks quakes and almost opposite direction for the Minto quake at the western side of ALPA (see Figures 15 through 19).

A general increase in amplitude with magnitude is indicated at least to a distance between 30 to 50 km from the epicenter. This is demonstrated by Figure 13 for stations 34, 24 and COL, where tilt amplitude versus magnitude is plotted. These particular stations are located in a narrow epicentral distance range (35.6 to 39 km for 24, 32.8 to 38.2 km for 34, 12 and 15 km for COL) except for the 10 Oct 70 mag. 3.2 quake (where 24 and 34 are near 51 km). The two shallower earthquakes indicate somewhat higher amplitude for 24 (two data points above full line, Figure 13) but not for 34, where the amplitude for the mag 2.9 quake is very low. For the dashed lines the log of amplitudes shows direct dependence on M, whereas for the full lines dependence is like M/1.5, a result in line with earlier findings by Berg and Pulpan (1970).

A cutoff magnitude for recording tilt steps seems at least indicated for 34 (at a distance near 35 km). Taking all data (of Figure 12) together it is not clearly possible to ascertain a dependence of a cutoff distance on Magnitude. Some cutoff between 40 and 50 km is, however, indicated by the reliable data, roughly at a distance twice the source depth.

CONCLUSION

Observed tilt steps often seem to be too large to be accommodated by existing theoretical dislocation models for a single layered homogeneous isotropic and elastic crust. Alternative solutions should be looked for in terms of more realistic crustal models and include plastic deformation in tectonically stressed areas, related to the nonlinear portion of the stress strain curve. This is partially indicated by the large tilt amplitude at short distances from the epicenter and by the observed low propagation velocity of tilt steps for local earthquakes in the Fairbanks area, and partially by the high tilt amplitudes associated with large distant earthquakes in the tectonically active area of Alaska.

LIST OF PUBLICATIONS, ACKNOWLEDGING AFOSR SUPPORT AND PAPERS GIVEN AT MEETINGS

L. Gedney, L. Shapiro, D. VanWormer and F. Weber: Earthquake Epicenters in Interior Alaska, 1968-1971 and Their Correlation with Mapped Faults. Geophysical Institute, University of Alaska, Research Report UAG R-218, March 1972a.

L. Gedney, L. Shapiro, D. VanWormer and F. Weber: Correlation of Epicenters with Mapped Faults East Central Alaska, 1968-1971. United States Department of Interior, Geological Survey, Open File Report, 1972b.

Eduard Berg and William Lutschak: Crustal Tilt Fields and Propagation Velocities Associated with Earthquakes. Presented: Royal Society Meeting, May 1972, to be published in short form in Proceedings, Royal Society.

E. Berg and W. Lutschak: Observations of Tiltfields, Propagation Velocities and Amplitude Die-Off Associated with Earthquakes. Presented 9th International Symposium on Geophysical Theory and Computers, Banff, Alberta, Canada, Aug 1972, to be published in the proceedings; Abstract in Program of the Symposium, University of Alberta, Aug. 1972.

REFERENCES

Berg, Eduard and Hans Pulpan, Tilts associated with small and medium size earthquakes, J. Physics Earth, 19, 59, 1971.

Chinnery, M. A., The deformation of the ground around surface faults, Bull. Seism. Soc. Amer., 51, 355, 1961.

Ewing, W. M., W. S. Jardetzky and Frank Press, Elastic Waves in Layered Media, McGraw-Hill, New York, 1957.

Gedney, Larry and Eduard Berg, The Fairbanks earthquake of June 21, 1967: Aftershock distribution, focal mechanisms and crustal parameters, Bull. Seism. Soc. Amer., 59, 73, 1969a.

Gedney, Larry and Eduard Berg, Some characteristics of the tectonic stress pattern in Alaska, Geophys. J. Royal Astron. Soc., 17, 293, 1969b.

Hanson, Kenneth, Eduard Berg and Larry Gedney, A seismic refraction profile and crustal structure in Central Interior Alaska, Bull. Seism. Soc. Amer., 58, 1657, 1968.

Kolsky, H., Stress Waves in Solids, Oxford, Clarendon Press, 1953.

Maue, A. W., Die Entspannungswelle bei plötzlichem Einschnitt eines gespannten elastischen Körpers, Zeits. ange. Math. Mechan., 34, 1, 1954.

Oliver, Jack, A summary of observed seismic surface wave dispersion, Bull. Seism. Soc. Amer., 52, 81, 1962.

Press, Frank, Displacements, strains and tilts at teleseismic distances, J. Geophys. Res., 70, 2395, 1965.

Sato, Ryosuke, Crustal deformation due to dislocation in a multi-layered medium, J. Physics Earth, 19, 31, 1971.

Stacey, F. D. and J. M. W. Rynn, Spurious local effects associated with teleseismic tilts and strains, in Earthquake Displacement Fields and the Rotation of the Earth (eds. L. Manshinha et al.), pp. 230-233, Dordrecht, Holland, D. Reidel Publishing Company, 1971.

Tocher, Don and P. L. Brown, Strain and tilt records of Cannikin, paper presented at the Annual Meeting of the Seismological Society of America, Honolulu 1972.

Wideman, C. J. and M. W. Major, Strainsteps associated with earthquakes, Bull. Seism. Soc. Amer., 57, 1429, 1967.

Romig, P. R., M. W. Major, C. J. Wideman and D. Tocher, Residual strains associated with a nuclear explosion, Bull. Seism. Soc. Amer., 59, No. 6, 2167-2176, 1969.

Date and location	Station	Tilt Amplitude (msec arc)		Total Amplitude (msec arc)	Total Amplitude (radians)	Est. Error (%)	Distance (km)	Magn.	Tilt Step Velocity (km/sec) S	Tilt Step Velocity (km/sec) Surface Wave	Record Type
10 January 1971	PAX	8.6N	32E	32.2	$15.6 \cdot 10^{-8}$	5	9,550	8.0	6.79	3.17 ± 0.1	Digital
New Guinea	MCK	*	18E	>18	$> 8.75 \cdot 10^{-8}$	10	9,408			E3.31	Tidal
	GLM	*	≤ 2E	≤ 2	$\le 0.9 \cdot 10^{-8}$		9,520				
26 March 1971	PAX	2.6S	12.5E	12.7	$6.2 \cdot 10^{-8}$	4	380	5.6-5.7		2.62 ± 0.1	Digital
S. Central Alaska											
11 May 1971	GLM	1.0N	2.7W	2.9	$1.4 \cdot 10^{-8}$		69	3.6		2.63 ± 0.1	Helicorder
Mioto											
9 July 1971	PAX	(2.2)N	<1.5	< 2.7	$< 1.3 \cdot 10^{-8}$		12,431				
Chile	MCK	(2.6)N	13.6E	13.9	$6.7 \cdot 10^{-8}$		12,625	7.5		3.62 ± 0.1	Tidal
	GLM	2-3N	<1	< 3	$< 1.4 \cdot 10^{-8}$		12,619				
14 July 1971	PAX	17.2N	21.4E	27.4	$13.3 \cdot 10^{-8}$		9,123			N3.68	Tidal
Solomon Islands	MCK	>16N	29.1E	>33.2	$>16.1 \cdot 10^{-8}$		9,017	7.7		E3.63	
										N3.18	
	GLM	< 5N	≈5E	< 7	$< 3.4 \cdot 10^{-8}$		9,153	7.8			
5 September 1971	PAX	2.9N	4.4W	5.3	$2.6 \cdot 10^{-8}$	25		7.1			
Sakhalin Island	MCK	9.1N	12.5E	15.5	$7.5 \cdot 10^{-8}$	10	4,570			EN 3.32	Tidal
	GLM	(<2)	≤2.3W	< 3	$< 1.4 \cdot 10^{-8}$	50					
4 January 1972	HIG	*	14W	14	$6.8 \cdot 10^{-8}$	20	8,160			3.74 + 0.1	Helicorder
Taiwan Region	GLM	<1 if any	**					6.8		(3.17)	Tidal (south)
	PAX	*	**					6.9			
	MCK	**	**								
29 February 1972	HIG	*	27W	27	$13.1 \cdot 10^{-8}$	20		7.2	5.78	3.55 ± 0.1	Helicorder
Japan Sea							6,170	7.1			
6 November 1971	Cape Sarichef				$< 4 \cdot 10^{-9}$	Strain	1,125			2.80 ± 0.1	Tucher and Brown chart at 40 mm/min
Amchitka					appr. $5 \cdot 10^{-10}$	Strain			(4.1-4.4)		Doubtful; too short a record
17 January 1968	Mt. Nebo	17.3S		17.3	$8.4 \cdot 10^{-8}$		1,910	5.3	4.6	3.77 ± 0.15	Stacey and Rynn 1 mm/min
E. New Guinea (near Brisbane)											

* = not available

**no offset = $< 5.10^{-9}$ or 1 msec

Table 2

10 October, 1970 earthquake ALPA amplitudes

SEISMOGRAM 112

CHANNEL A21 HAS A RANGE OF .5000 AND 5.9477E 02 MU.
CHANNEL 321 HAS A RANGE OF .5000 AND 8.1321E 02 MU.
CHANNEL 331 HAS A RANGE OF .5000 AND 1.0885E 03 MU.
CHANNEL A31 HAS A RANGE OF .5000 AND 4.9826E 03 MU.
CHANNEL 341 HAS A RANGE OF .5000 AND 1.5880E 03 MU.
CHANNEL 231 HAS A RANGE OF .5000 AND 6.2879E 02 MU.
CHANNEL 311 HAS A RANGE OF .5000 AND 4.0489E 06 MU.
CHANNEL 111 HAS A RANGE OF .5000 AND 1.9134E 03 MU.
CHANNEL 241 HAS A RANGE OF .5000 AND 6.3482E 02 MU.

SEISMOGRAM 113

CHANNEL A22 HAS A RANGE OF .5000 AND 9.3269E 02 MU.
CHANNEL 322 HAS A RANGE OF .5000 AND 8.0131E 02 MU.
CHANNEL 332 HAS A RANGE OF .5000 AND 2.2959E 03 MU.
CHANNEL A32 HAS A RANGE OF .5000 AND 3.3191E 03 MU.
CHANNEL 342 HAS A RANGE OF .5000 AND 2.2698E 03 MU.
CHANNEL 232 HAS A RANGE OF .5000 AND 3.9932E 02 MU.
CHANNEL 312 HAS A RANGE OF .5000 AND 2.8573E 06 MU.
CHANNEL 112 HAS A RANGE OF .5000 AND 1.3593E 03 MU.
CHANNEL 242 HAS A RANGE OF .5000 AND 5.0524E 02 MU.

SEISMOGRAM 114

CHANNEL A23 HAS A RANGE OF .5000 AND 1.1429E 03 MU.
CHANNEL 323 HAS A RANGE OF .5000 AND 4.6280E 02 MU.
CHANNEL 333 HAS A RANGE OF .5000 AND 1.4806E 03 MU.
CHANNEL A33 HAS A RANGE OF .5000 AND 6.0082E 03 MU.
CHANNEL 343 HAS A RANGE OF .5000 AND 3.7330E 01 MU.
CHANNEL 233 HAS A RANGE OF .5000 AND 2.1723E 02 MU.
CHANNEL 313 HAS A RANGE OF .5000 AND 4.9522E 06 MU.
CHANNEL 113 HAS A RANGE OF .5000 AND 2.3678E 03 MU.
CHANNEL 243 HAS A RANGE OF .5000 AND 3.5554E 02 MU.

LIST OF FIGURES

Figure 10. Tilt arrival times after origin time versus focal distance for four Fairbanks earthquakes. Station identification given by numbers and/or letters.

Figure 11. a.) b.) Total tilt amplitude versus epicentral distance values in ( ) are uncertain or possible maximum. Stations with the same subsymbol (horizontal or vertical lines) are located in or nearly in line with the epicenter. Plots are ordered by decreasing magnitude.

Figure 12. Summary plot of previous Figure 11a and b.

Figure 13. Tilt amplitude versus magnitude for stations 34, 24 and COL; each station is at a comparable epicenter distance for all quakes, and focal distance was also nearly equal except for 2 quakes (see text).

Figure 14. a.) Vertical ALPA outputs for 10 October 1970 quake. The first two letters and/or numbers are station identification.

Figure 14. b.) E-W ALPA outputs for 10 October 1970 quake leading to tilts indicated in Figure 19. For amplitudes refer to Table 2.

Figure 14. c.) N-S ALPA outputs for 10 October 1970 quake.

Figure 15. Normalized ALPA station outputs, tilt directions and tilt amplitudes (including GLM and COL) for the 1 May 1971 quake. For comparison with calibration pulse refer to text. The length of tilt arrow has to be multiplied by the factor indicated to correspond to scale.

Figure 16. Tilt direction and amplitude for the 11 May 1971 quake. The length of the arrow has to be multiplied by the factor indicated to correspond to scale.

Figure 17. Tilt direction and amplitudes for the 13 May 1971 quake. The length of the arrow has to be multiplied by the factor indicated to correspond to scale.

Figure 18. Tilt direction and amplitudes for the 10 October 1970 quake. The length of the arrow has to be multiplied by the factor indicated to correspond to scale. The original data are presented in Figure 14 and amplitudes are given in Table 2.

Figure 19. Tilt direction and amplitude for the 12 November 1970 quake. The length of the arrow has to be multiplied by the factor indicated to correspond to scale.

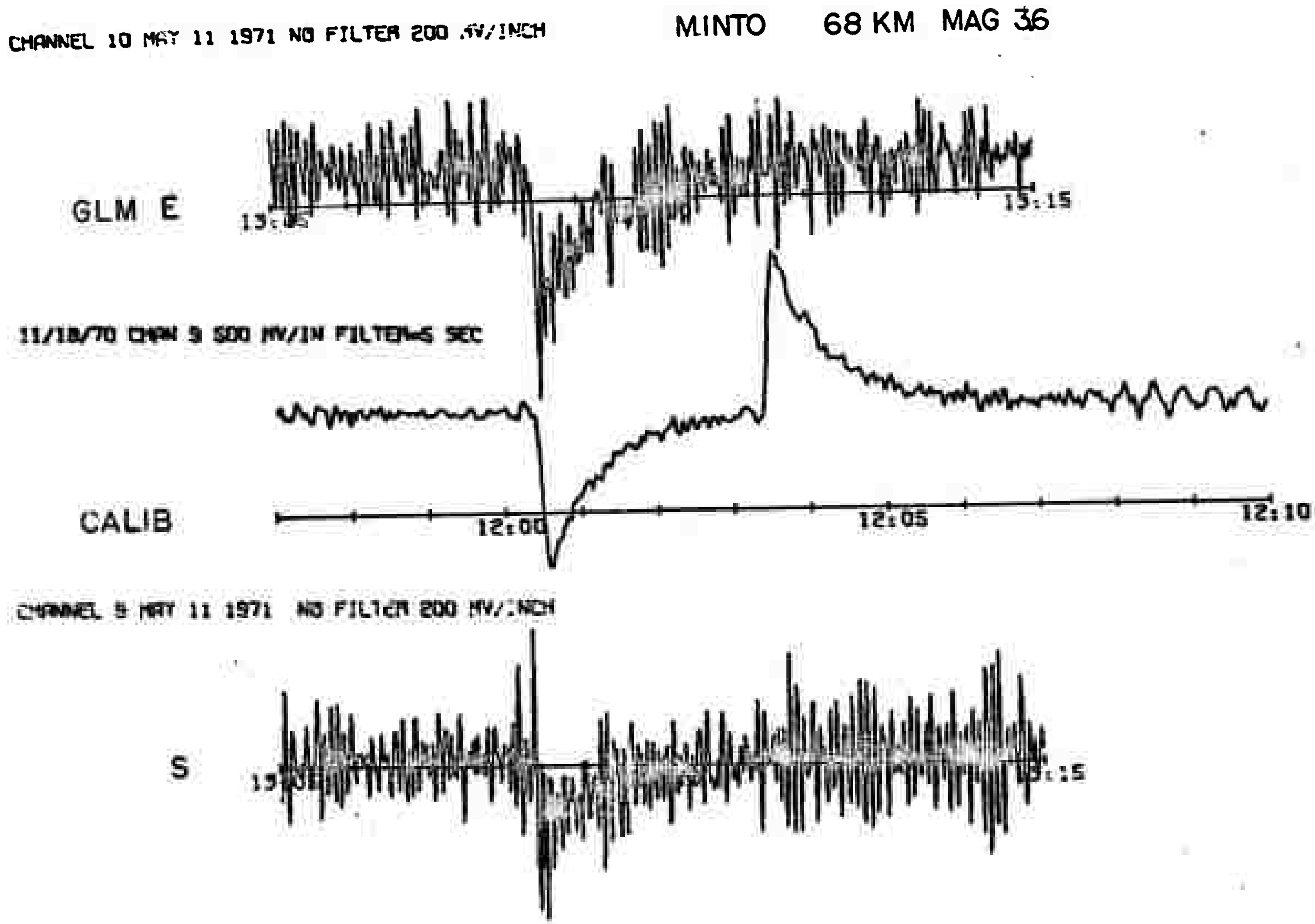

Fig. I Glm LP digital records from Minto earthquake unfiltered; Calibration pulse box car filtered at 5 seconds. Up on records is: Groundmotion W and N; Tilt E and S. Original scale was 3/4 inch per minute.

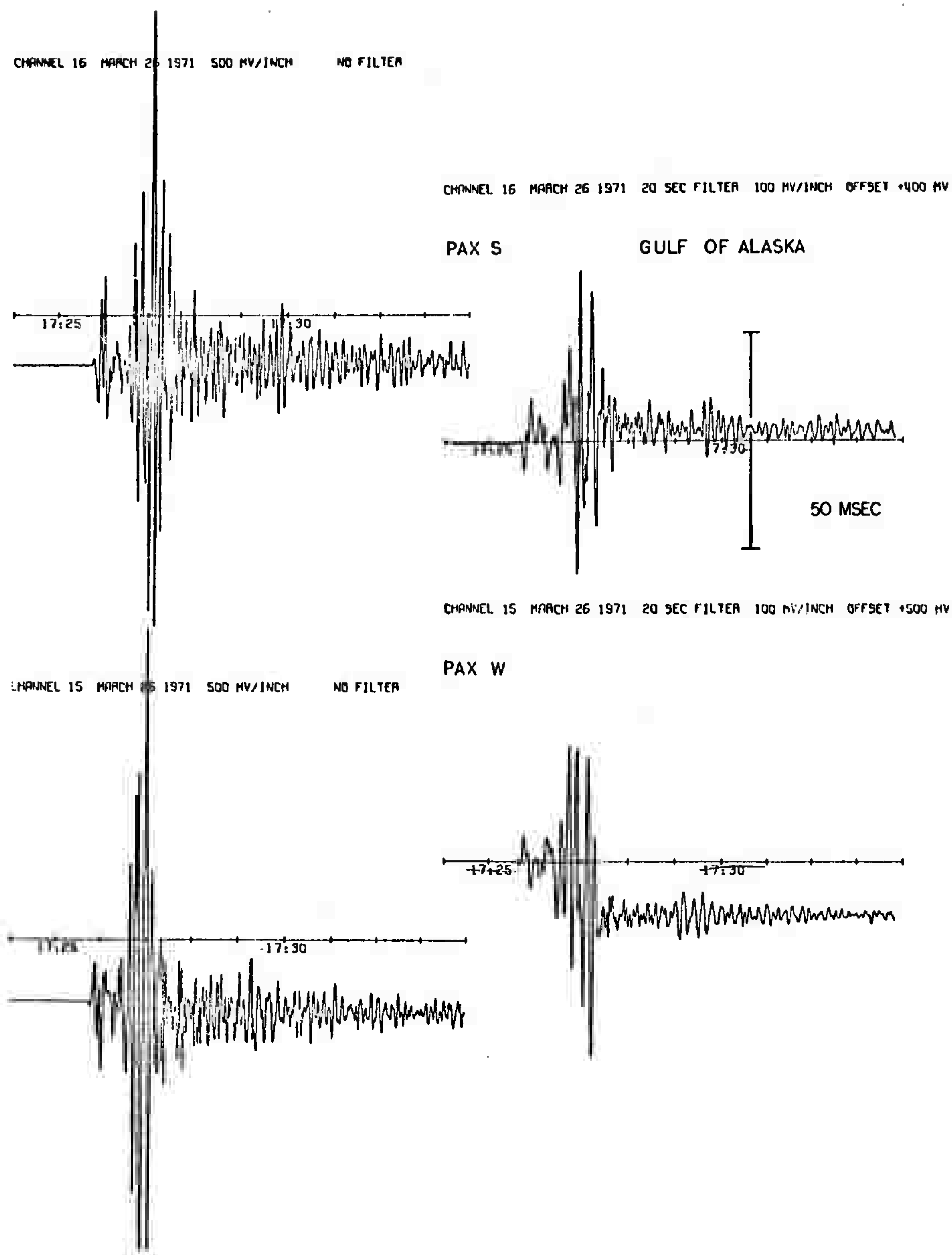

Fig. 2 PAX digital records from an earthquake in the Gulf of Alaska. Left side unfiltered data, right side sensitivity is increased five times and data are box car filtered at 20 sec. Notice tilt offset towards the southeast. Time scale on original records is 3/4 inch per minute. Indicated time is not correct.

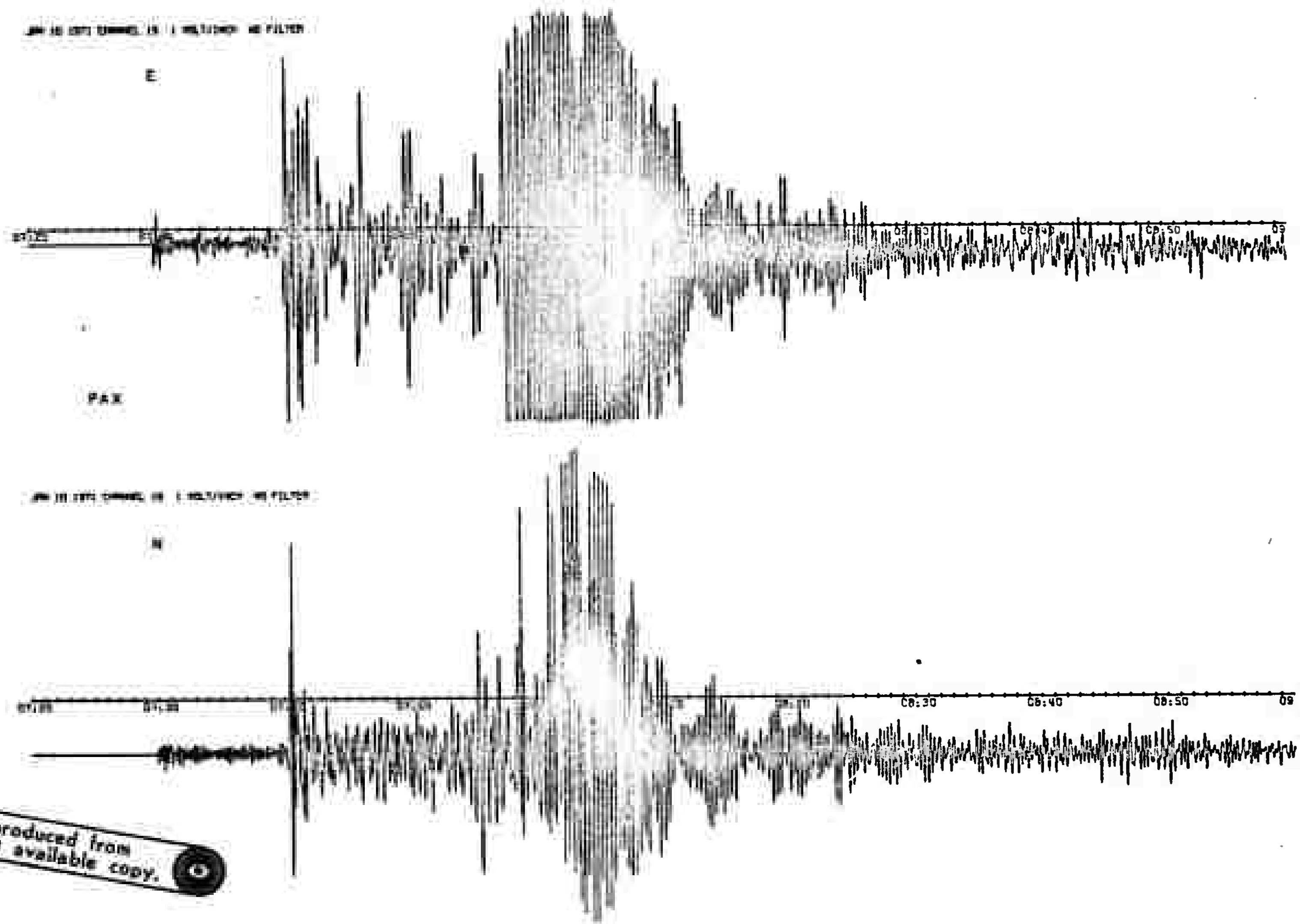

Fig. 3 Unfiltered digital data, PA?, for the New Guinea quake of IO January, I97I, distance over 9000 km, original time scale I/4 inch per minute. Compare to next figure.

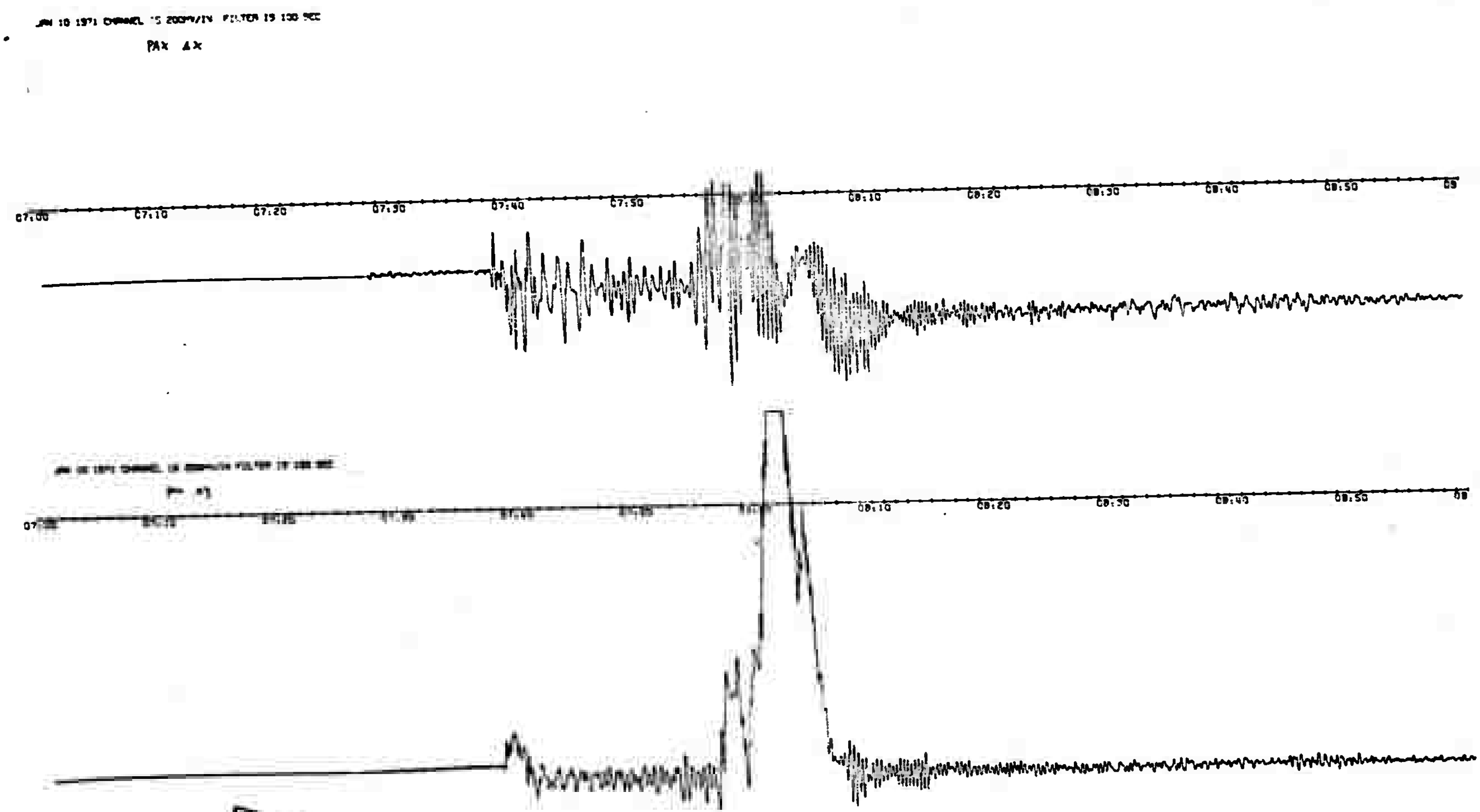

Fig. 4 PAX record of New Guinea earthquake 10 January, 1971 box car filtered at 100 sec and 5 times increased sensitivity from previous figure. Notice the first tilt offset near 07ʰ40 toward N-E and the second near 08ʰ08. Propagation velocity of the second tilt is 3.15 $\pm$ 0.1 km/sec. Compare also to next figure.

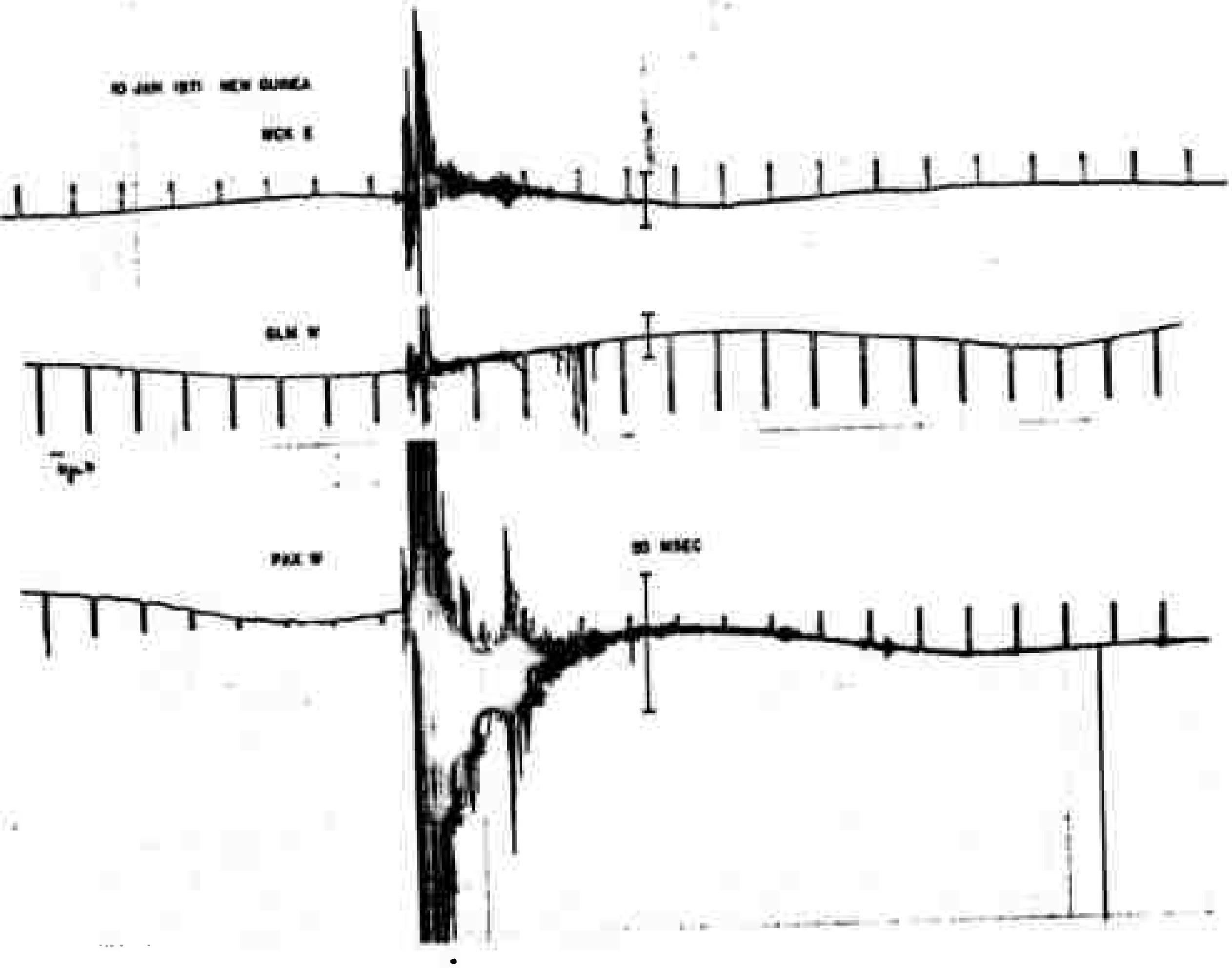

Fig. 5 E-W tilt record of the January 10, 1971 Guinea earthquake, recorded at MCK, GLM, and PAX. The difference in amplitude results from the difference in operation: MCK was directly recorded at the station, GLM was telemetered and (R-C) filtered at a 30 sec corner period. Both traces are feedback signals. PAX is the transducer output (no feedback applied), telemetered and recorded after a (R-C) 30 sec corner period filter. "0" reference marks are spaced I hour apart. Up on record is tilt toward the indicated direction, and the bares correspond to 50 msec arc.

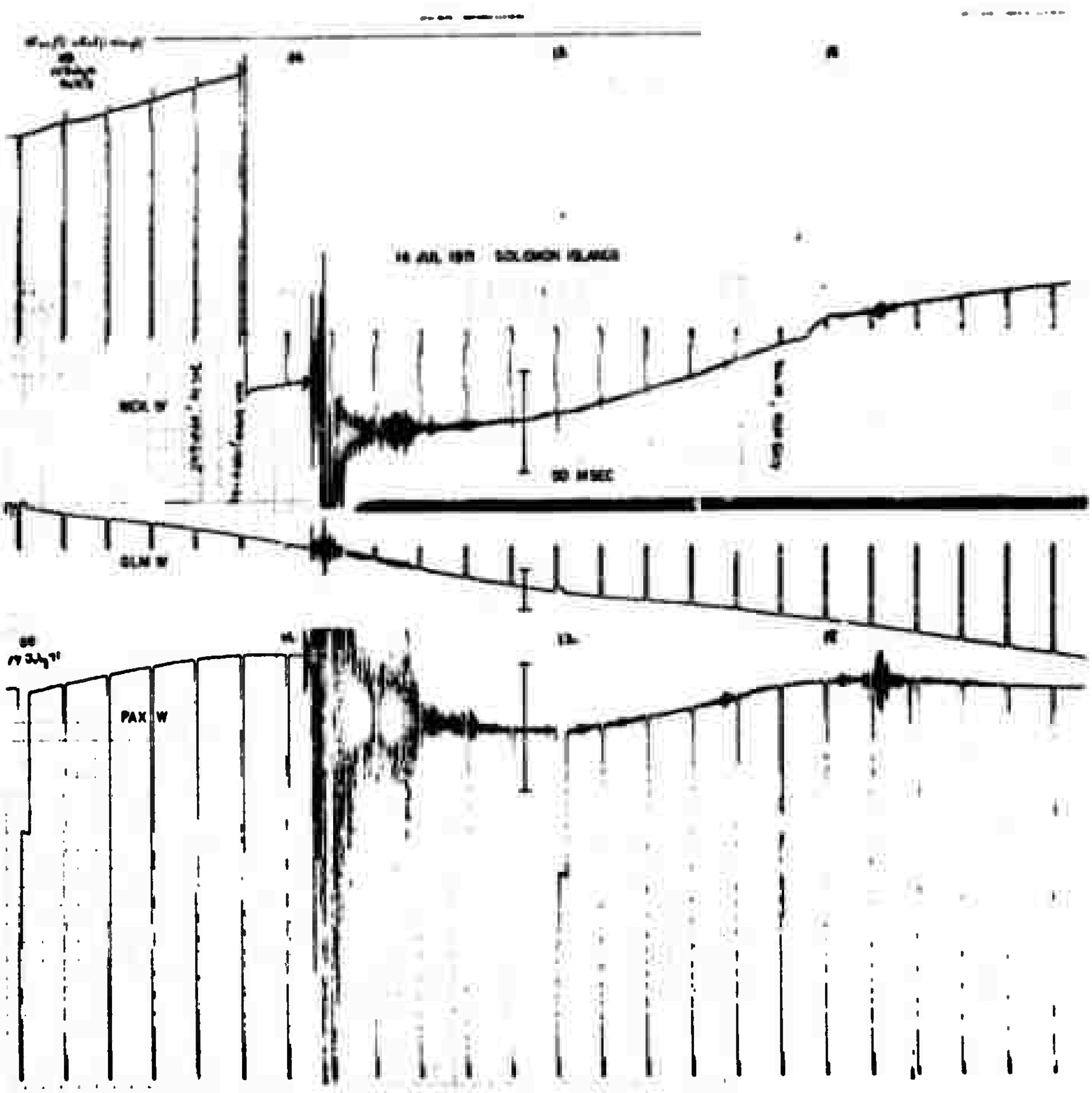

Fig. 6 14 July, 1971 Solomon Island earthquake. E-W tilt records. Compare the very similar tilts during the New Guinea earthquake in the preceeding figure. Note however that recording polarity for MCK is reversed, but tilt direction is not. Other details as in figure 5.

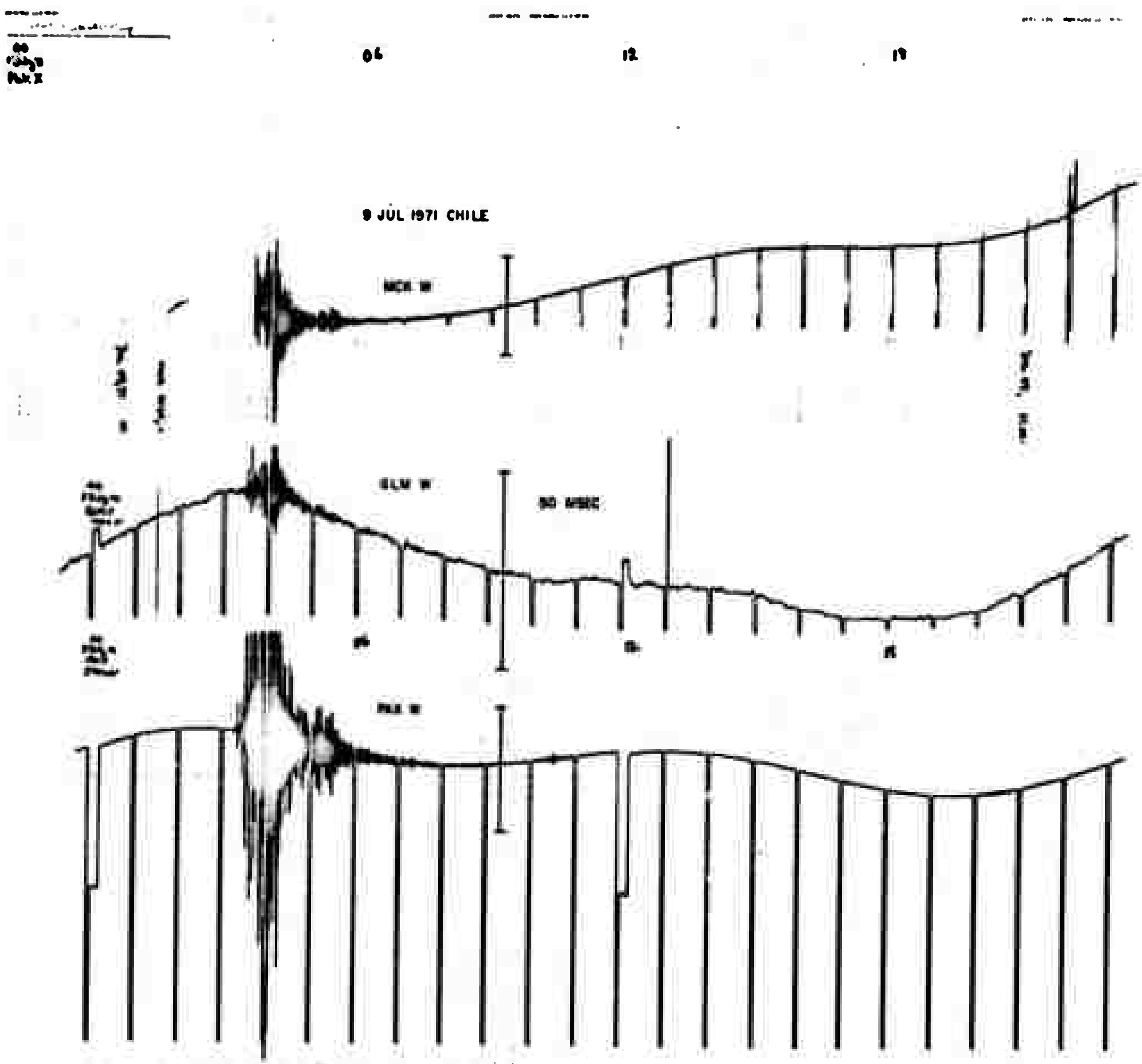

Fig. 7 9 July, 1971 Chile earthquake, E-W tilt records. For other details refer to figure 5.

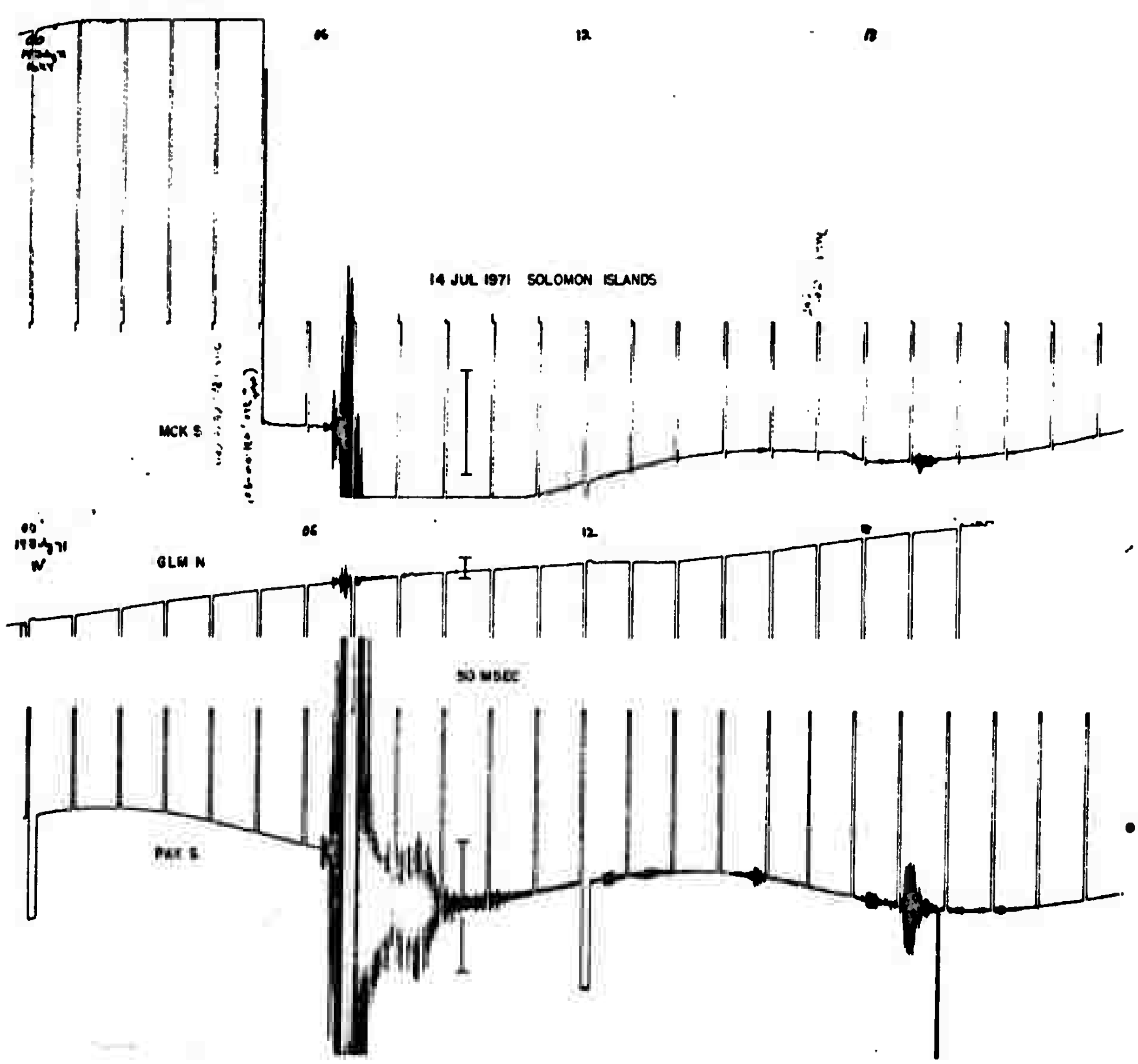

Fig. 8 14 July, 1971 Solomon Island N-S tilt records. For other details refer to figure 5.

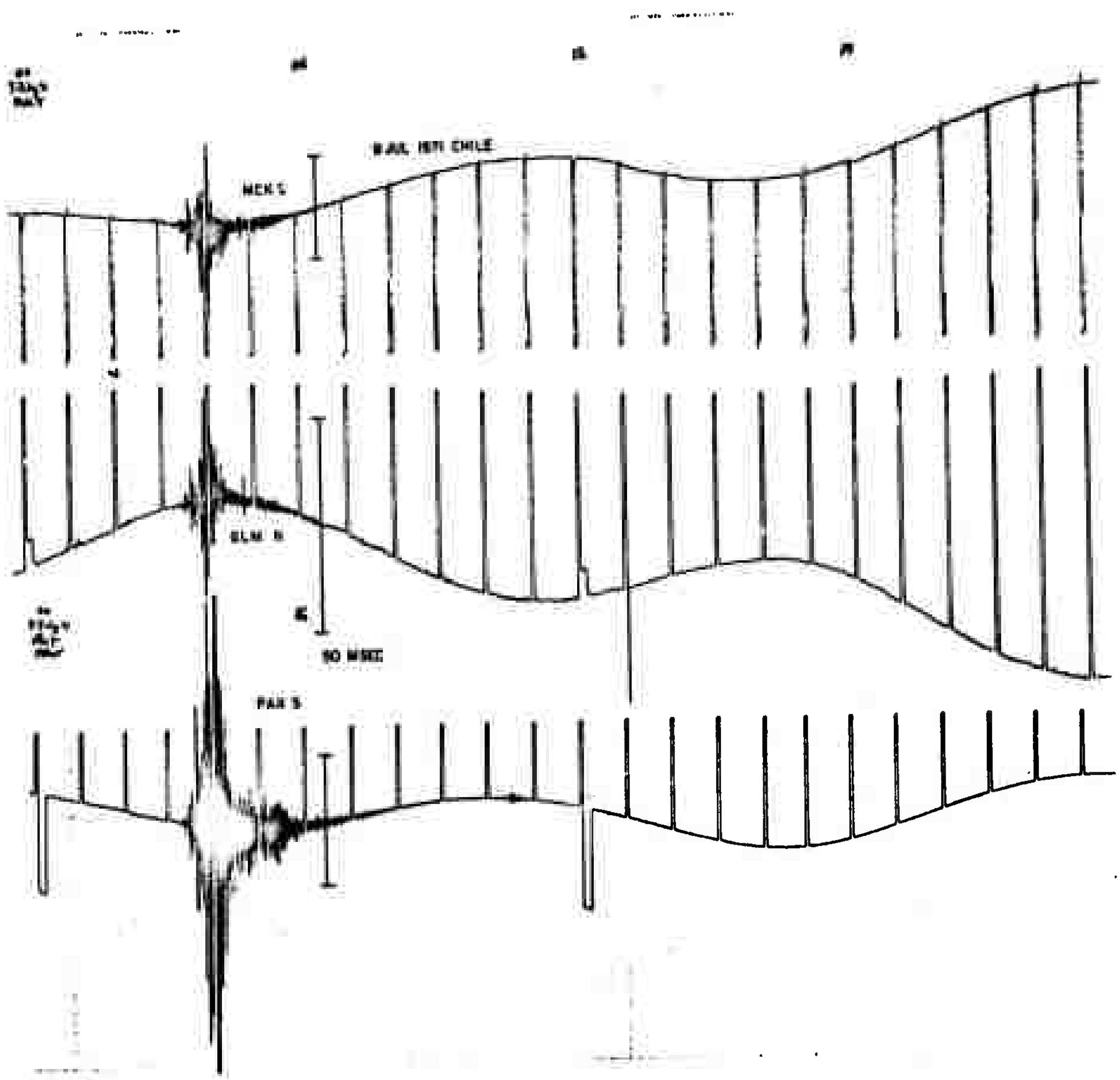

Fig. 9 9 July, 1971 Chile earthquake N-S tilt records. For other details refer to figure 5.

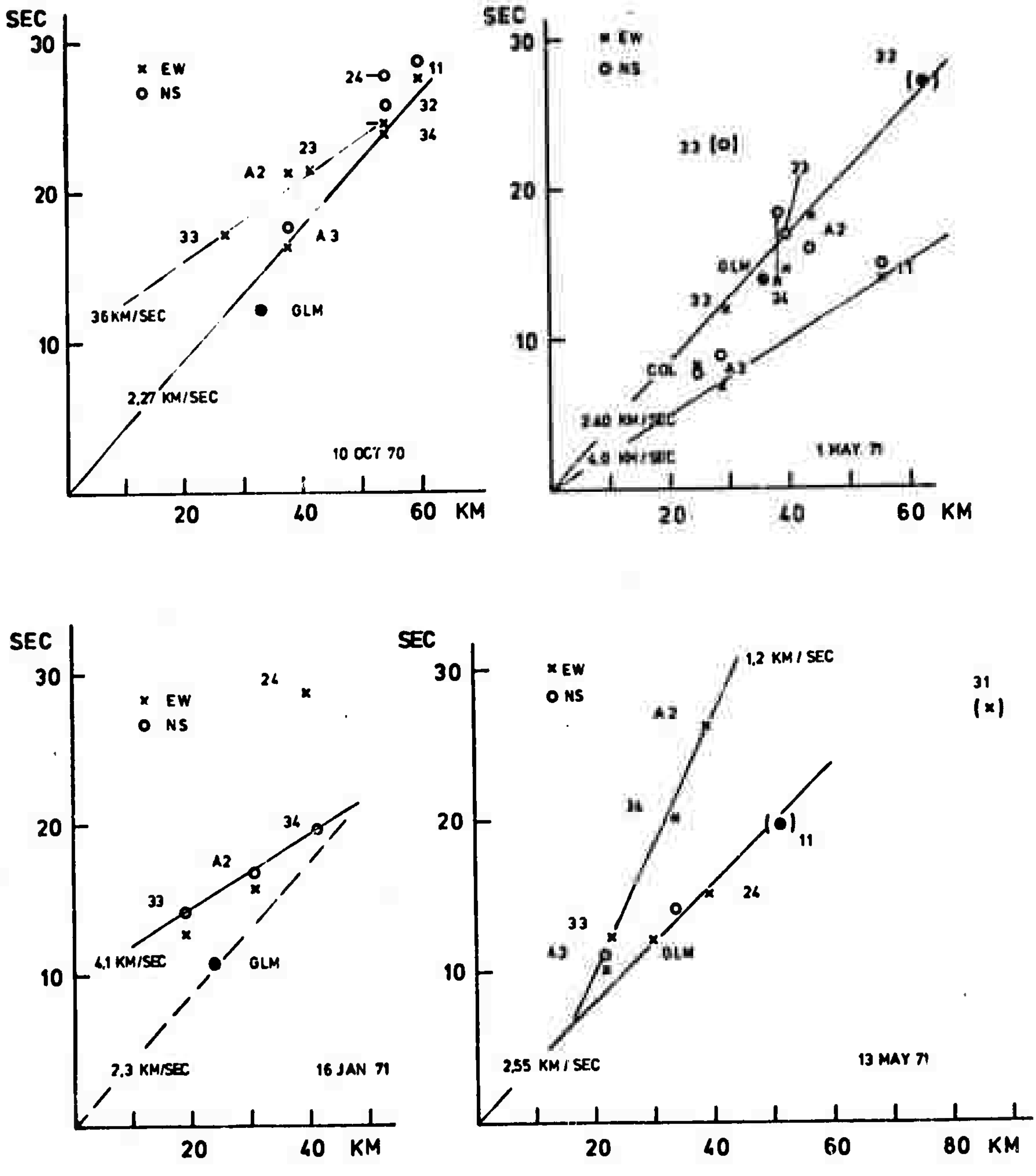

Fig. 10 Tilt arrival times after origin time versus focal distance for four Fairbanks earthquakes. Station identification given by numbers and/or letters.

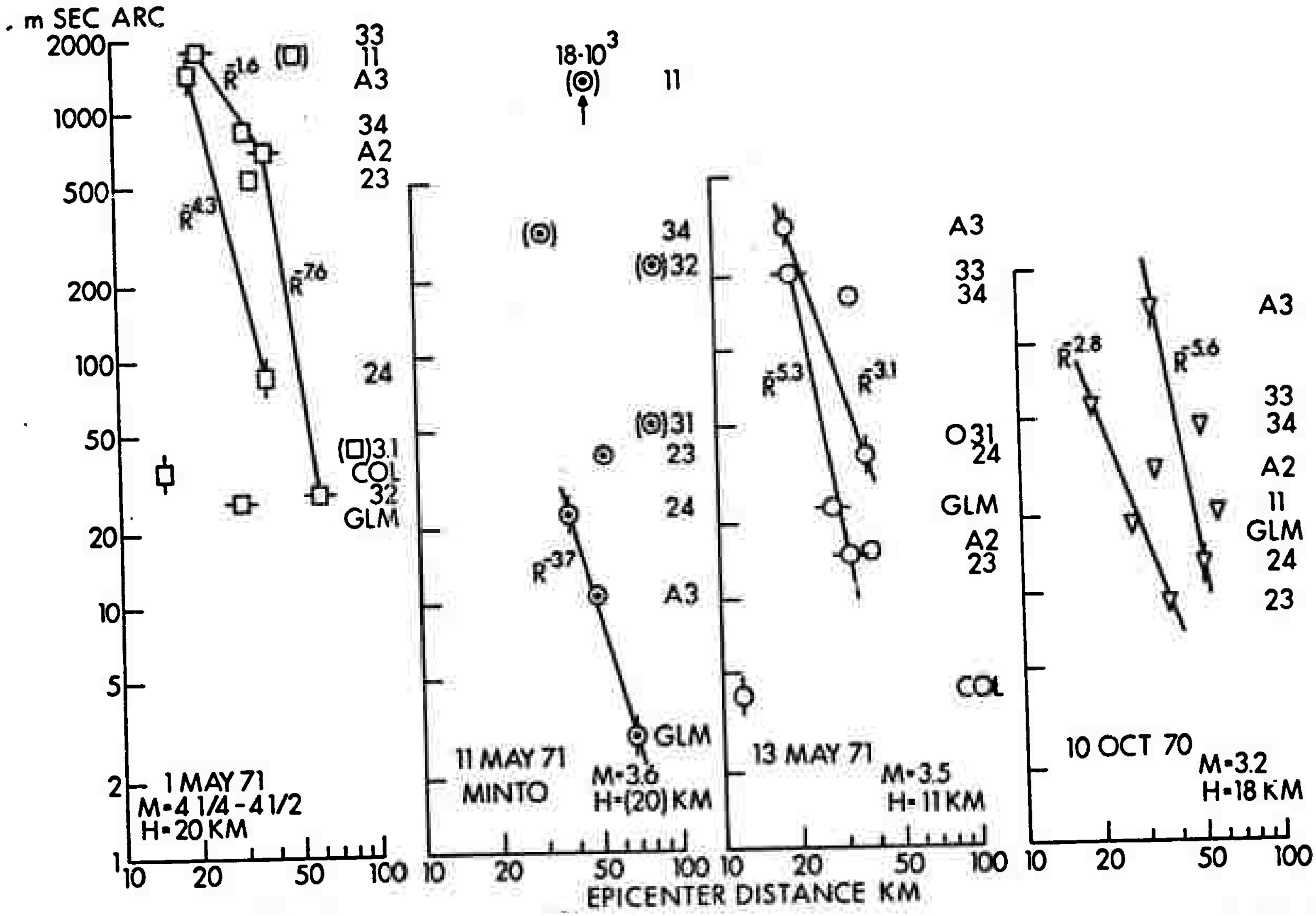

Fig. 11 a.) Total tilt amplitude versus epicentral distance values in () are uncertain or possible maximum. Stations with the same subsymbol (horizontal or vertical lines) are located in or nearly in line with the epicenter. Plots are ordered by decreasing magnitude.

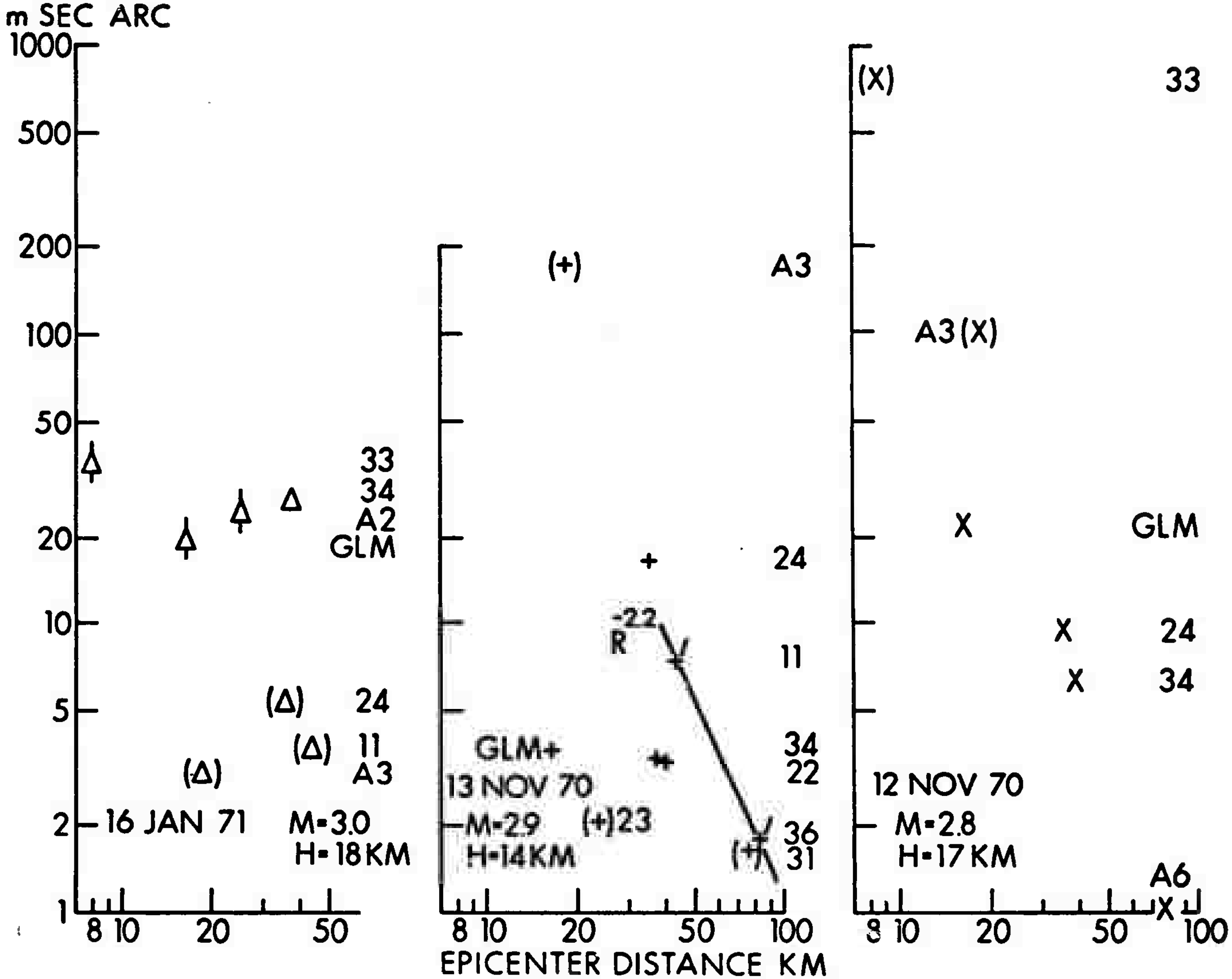

Fig. 11 b.) Total tilt amplitude versus epicentral distance values in () are uncertain or possible maximum. Stations with the same subsymbol (horizontal or vertical lines) are located in or nearly in line with the epicenter. Plots are ordered by decreasing magnitude.

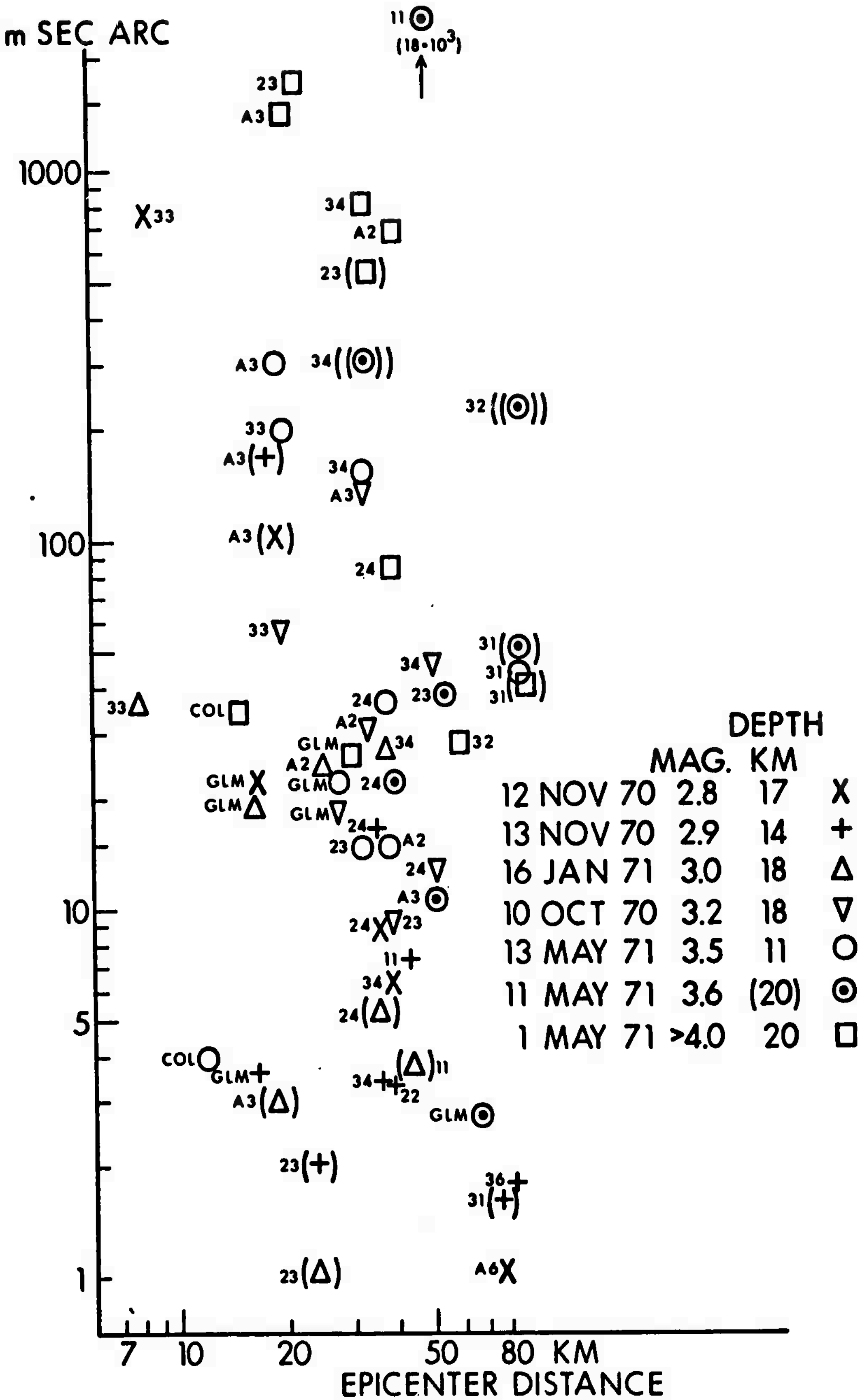

39

Fig. I2 Summary plot of previous Figure II a and b.

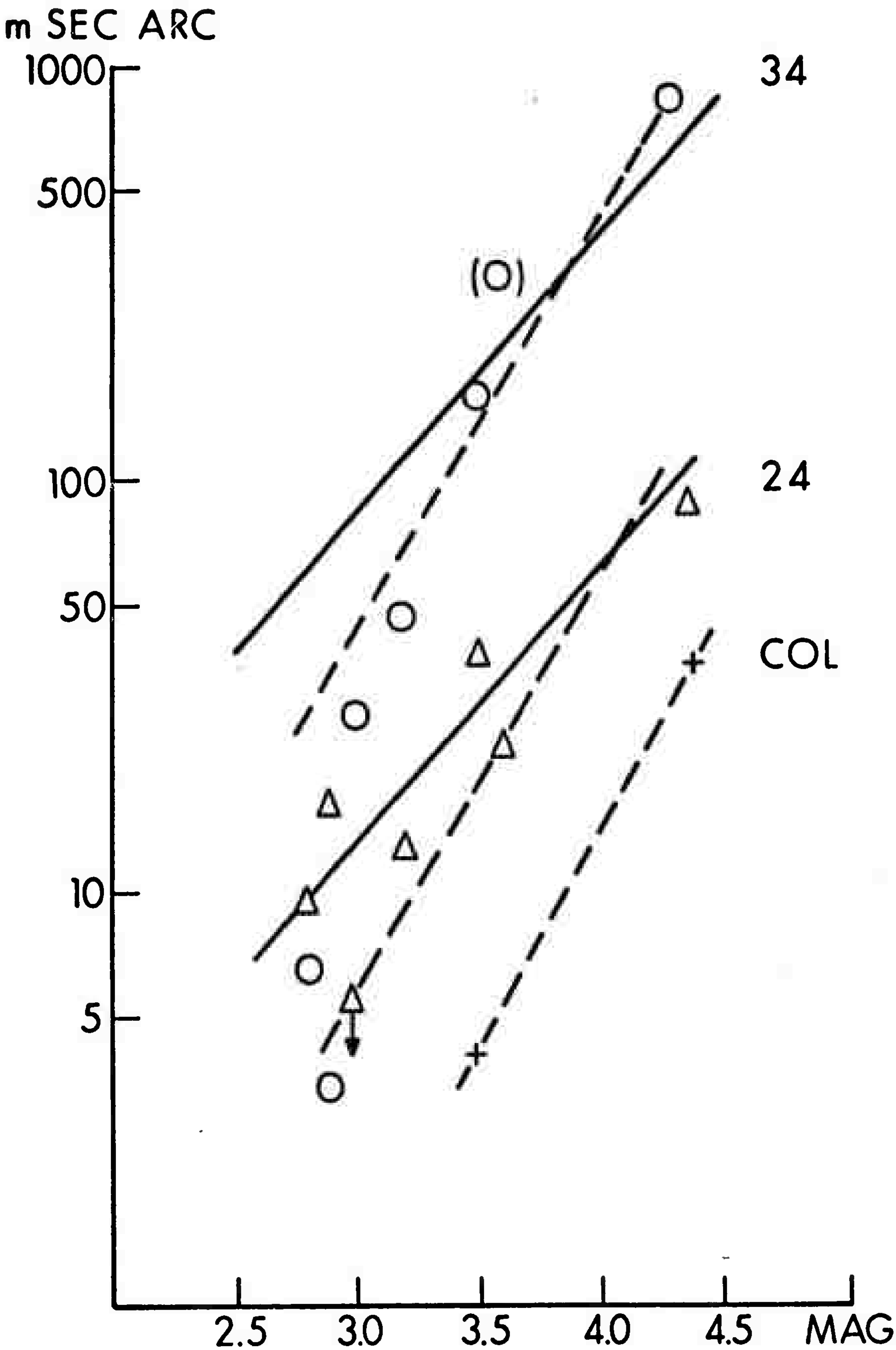

Fig. 13 Tilt amplitude versus magnitude for stations 34, 24 and COL. Each station is at a comparable epicenter distance for all quakes, and focal distance was also nearly equal except for 2 quakes (see text).

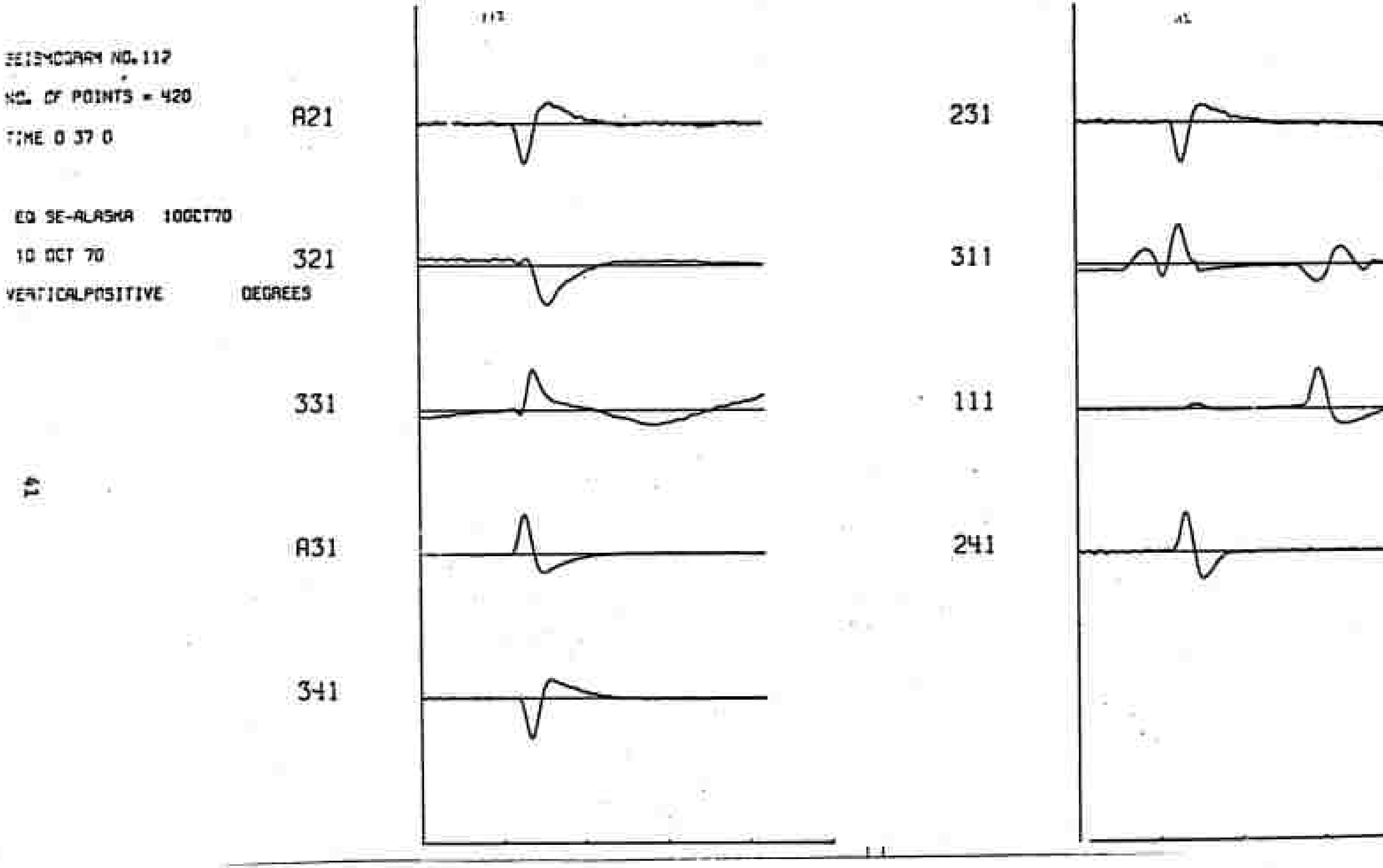

Fig. I4 a.) Vertical ALPA outputs for IO October, I970 quake. The first two letters and/or numbers are station identification.

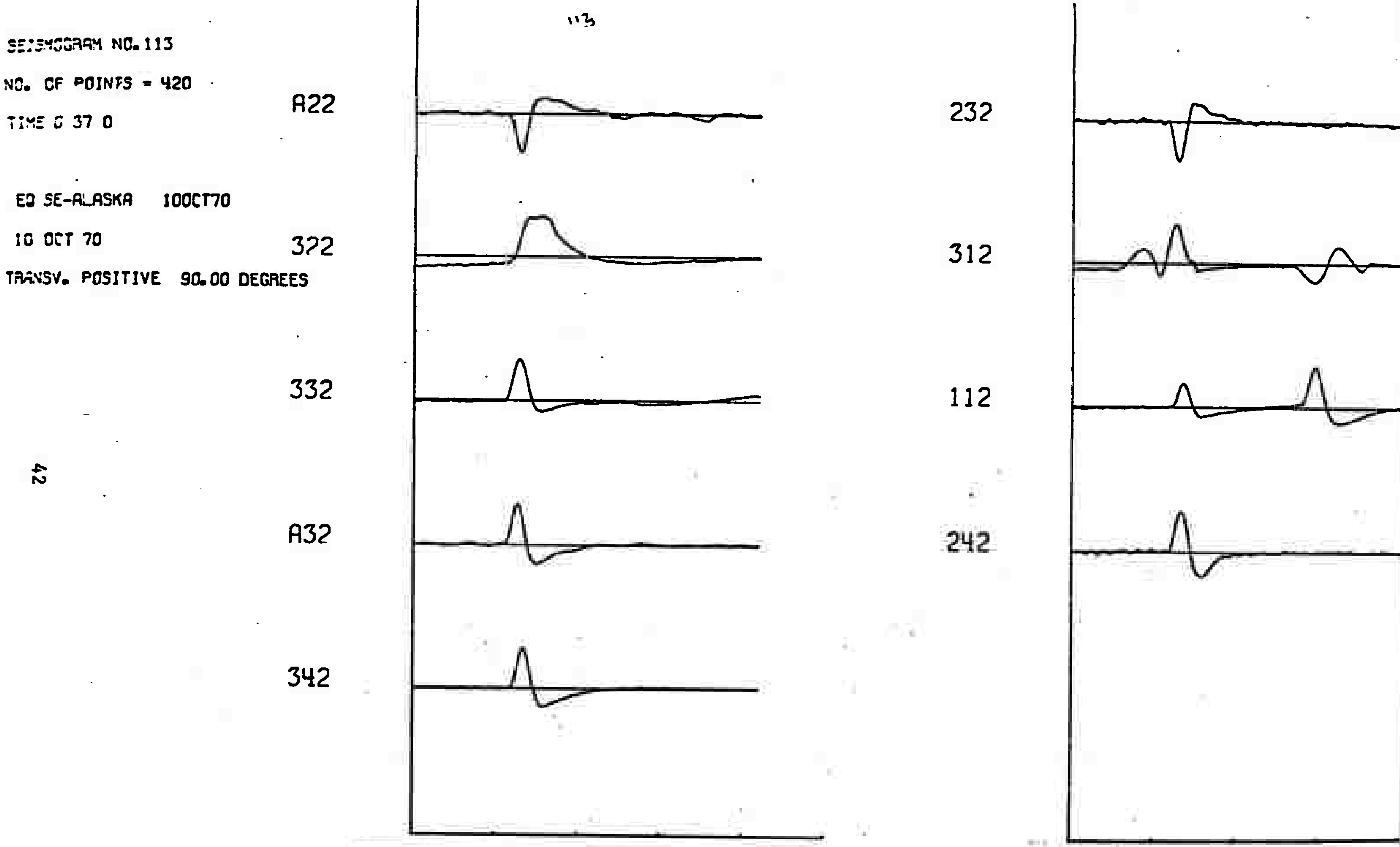

Fig. I4 b.) E-W ALPA outputs for IO October, I970 quake leading to tilts indicated in Fig. I9. For amplitudes refer to Table 2.

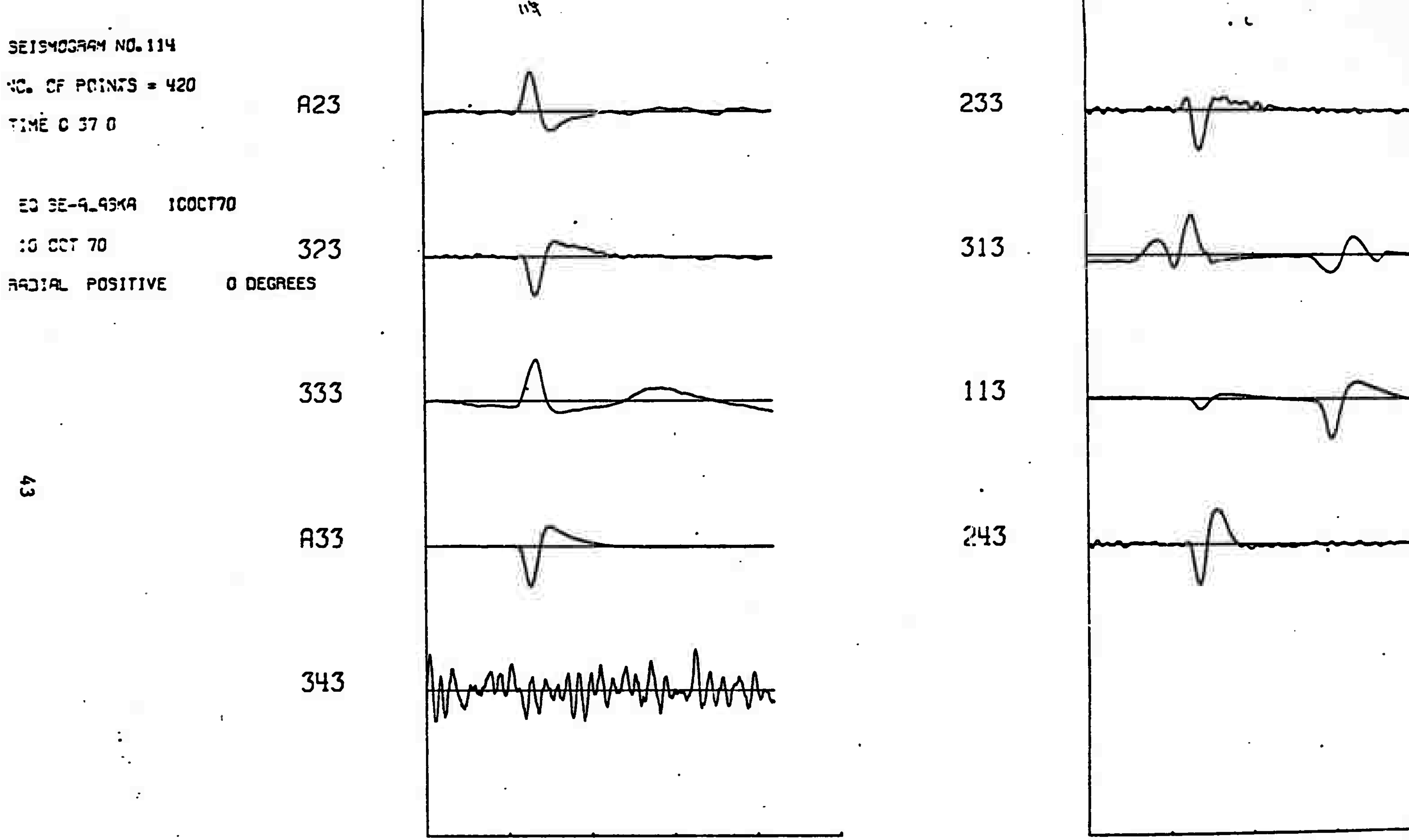

Fig. I4 c.) N-S ALPA outputs for I0 October, I970 quake.

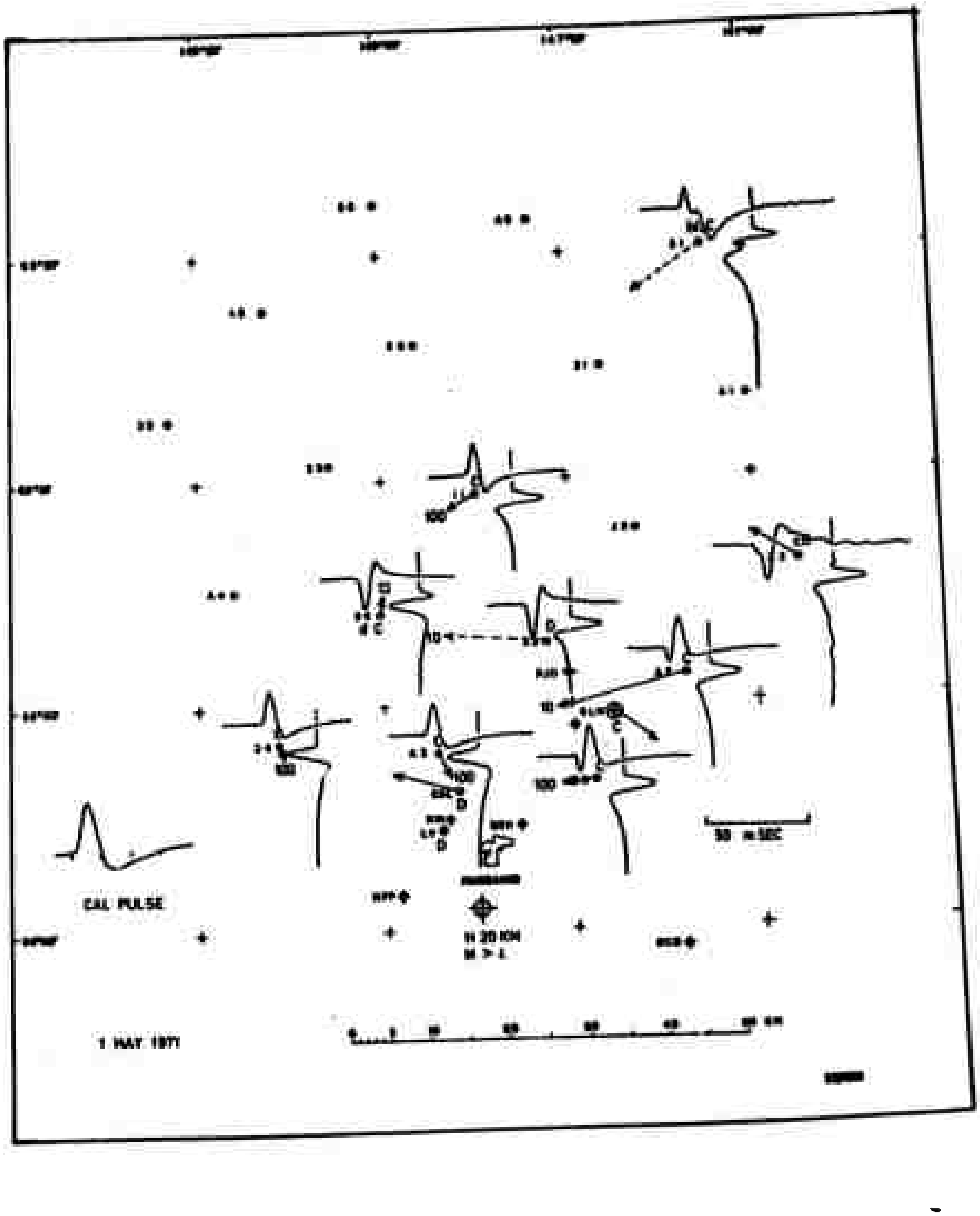

Fig. I5 Normalized ALPA station outputs, tilt directions and tilt amplitudes (including GLM and COL) for the I May, I97I quake. For comparison with calibration pulse refer to text. The length of tilt arrow has to be multiplied by the factor indicated to correspond to scale.

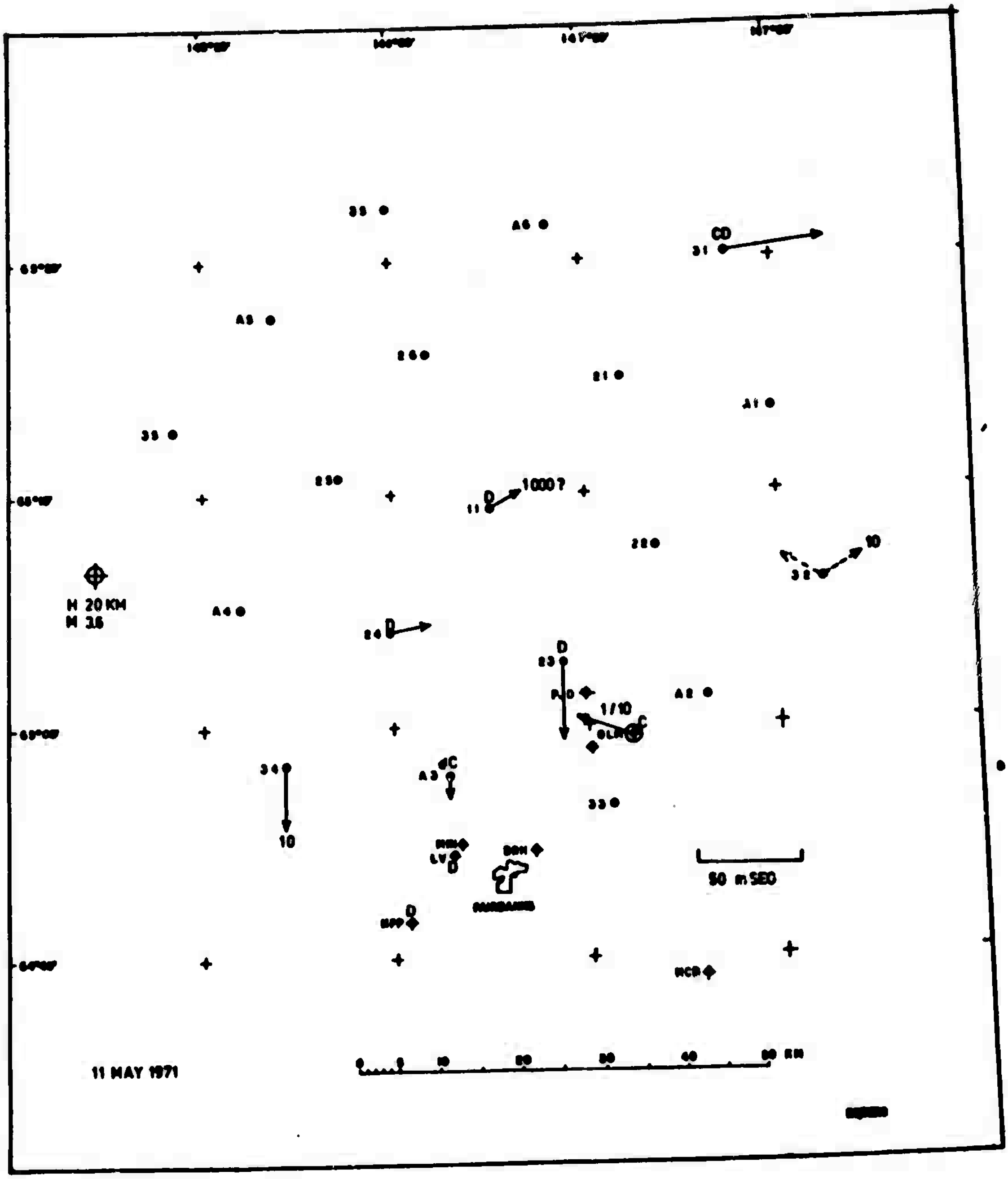

Fig. I6 Tilt direction and amplitude for the II May, I97I quake. The length of the arrow has to be multiplied by the factor indicated to correspond to scale.

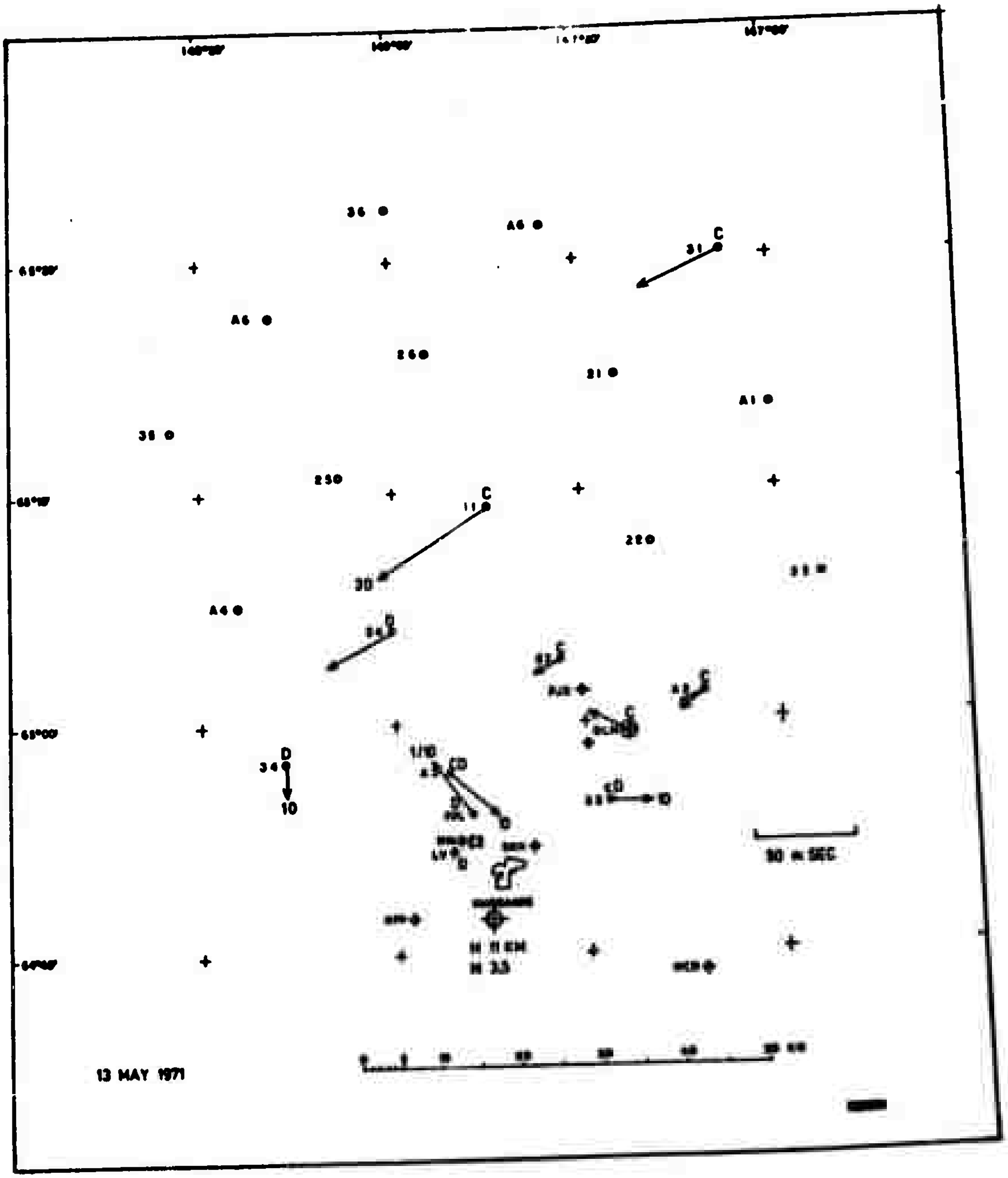

Fig. 17 Tilt direction and amplitudes for the 13 May, 1971 quake. The length of the arrow has to be multiplied by the factor indicated to correspond to scale.

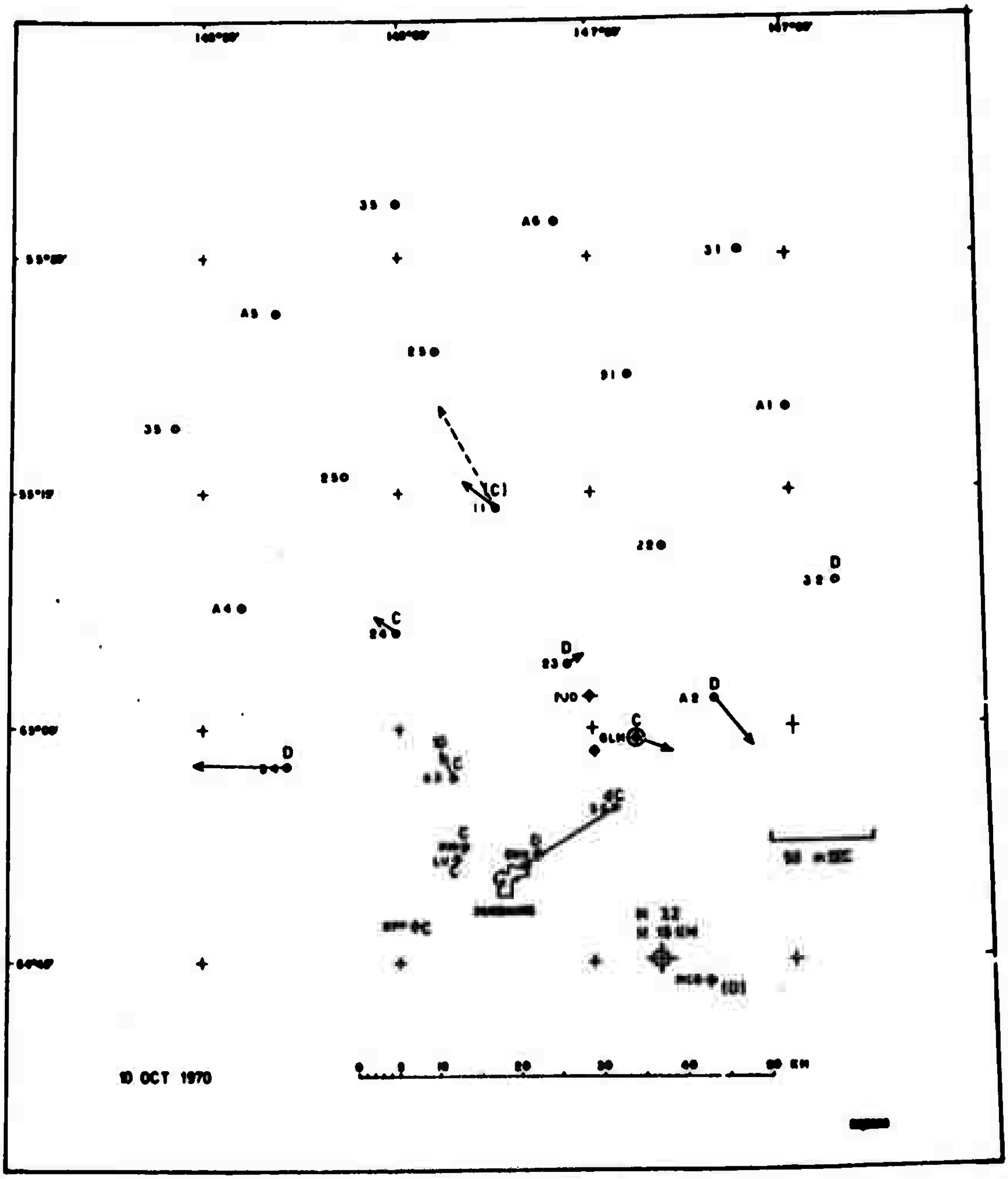

Fig. 18 Tilt direction and amplitudes for the 10 October, 1970 quake. The length of the arrow has to be multiplied by the factor indicated to correspond to scale. The original data are presented in Fig.14 and amplitudes are given in Table 2.

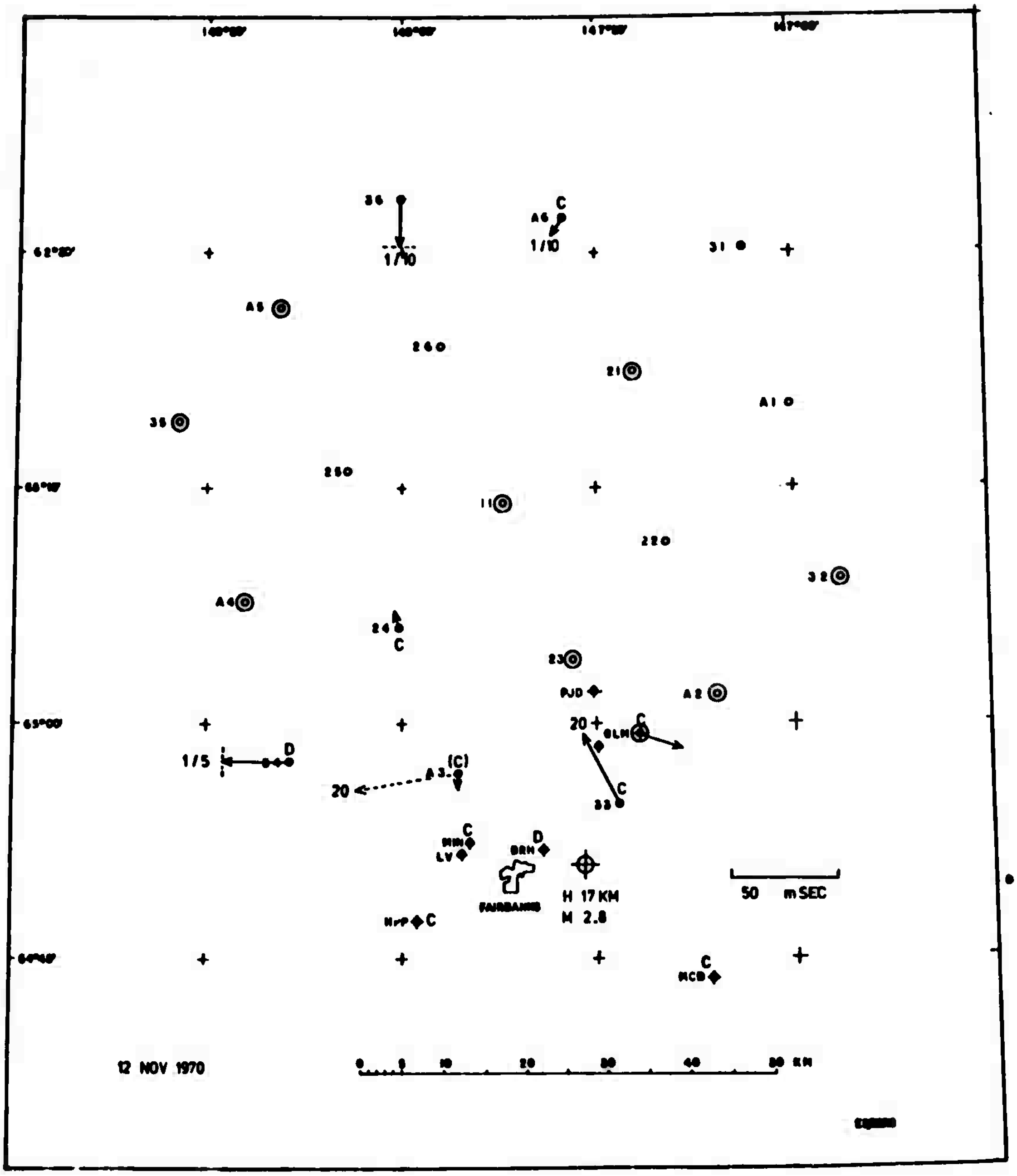

Fig. I9 Tilt direction and amplitude for the I2 November, I970 quake. The length of the arrow has to be multiplied by the factor indicated to correspond to scale.